





bFGF-Chitosan “brain glue” promotes functional recovery after cortical ischemic stroke

Jiao Mu^{a,b,c,1}, Xiang Zou^{d,1} , Xinjie Bao^{e,1}, Zhaoyang Yang^{b,1}, Peng Hao^b, Hongmei Duan^b, Wen Zhao^b, Yudan Gao^b, Jinting Wu^f, Kun Miao^b, Kwok-Fai So^{g,h,i,j,k,****}, Liang Chen^{d,***}, Ying Mao^{d,**}, Xiaoguang Li^{a,b,*} 

^a Beijing Key Laboratory for Biomaterials and Neural Regeneration, Beijing Advanced Innovation Center for Biomedical Engineering, School of Biological Science and Medical Engineering, Beihang University, Beijing 100083, China

^b Department of Neurobiology, School of Basic Medical Sciences, Capital Medical University, Beijing, 100069, China

^c Department of Pathology, Hebei North University, No. 11 Zuanshan Road, Zhangjiakou, Hebei, 075000, China

^d Department of Neurosurgery, Huashan Hospital, Fudan University, No. 12 Wulumuqi Zhong Road, Shanghai, 200040, China

^e Department of Neurosurgery, Peking Union Medical College Hospital, Chinese Academy of Medical Sciences and Peking Union Medical College, Beijing, China

^f Department of Neurosurgery, Yuquan Hospital, School of Medicine, Tsinghua University, Beijing, China

^g Guangdong-Hongkong-Macau Institute of CNS Regeneration, Ministry of Education CNS Regeneration Collaborative Joint Laboratory, Jinan University, 510632, Guangzhou, Guangdong Province, China

^h Bioland Laboratory (Guangzhou Regenerative Medicine and Health Guangdong Laboratory), 510530, Guangzhou, Guangdong Province, China

ⁱ Department of Ophthalmology and State Key Laboratory of Brain and Cognitive Sciences, The University of Hong Kong, 999077, China

^j Center for Brain Science and Brain-Inspired Intelligence, Guangdong-Hong Kong-Macao, Greater Bay Area, 510515, Guangzhou, Guangdong Province, China

^k Co-innovation Center of Neuroregeneration, Nantong University, 226001, Nantong, Jiangsu Province, China

ARTICLE INFO

Keywords:

bFGF-Chitosan gel
Ischemic stroke
New-born neurons
Angiogenesis
Synaptogenesis
Neural circuit reconstruction

ABSTRACT

The mammalian brain has an extremely limited ability to regenerate lost neurons and to recover function following ischemic stroke. A biomaterial strategy of slowly-releasing various regeneration-promoting factors to activate endogenous neurogenesis represents a safe and practical neuronal replacement therapy. In this study, basic fibroblast growth factor (bFGF)-Chitosan gel is injected into the stroke cavity. This approach promotes the proliferation of vascular endothelial cell, the formation of functional vascular network, and the final restoration of cerebral blood flow. Additionally, bFGF-Chitosan gel activates neural progenitor cells (NPCs) in the sub-ventricular zone (SVZ), promotes the NPCs' migration toward the stroke cavity and differentiation into mature neurons with diverse cell types (inhibitory gamma-aminobutyric acid neurons and excitatory glutamatergic neuron) and layer architecture (superficial cortex and deep cortex). These new-born neurons form functional synaptic connections with the host brain and reconstruct nascent neural networks. Furthermore, synaptogenesis in the stroke cavity and Nestin lineage cells respectively contribute to the improvement of sensorimotor function induced by bFGF-Chitosan gel after ischemic stroke. Lastly, bFGF-Chitosan gel inhibits microglia activation in the peri-infarct cortex. Our findings indicate that filling the stroke cavity with bFGF-Chitosan “brain glue” promotes angiogenesis, endogenous neurogenesis and synaptogenesis to restore function, offering innovative ideas and methods for the clinical treatment of ischemic stroke.

* Corresponding authors. Beijing Key Laboratory for Biomaterials and Neural Regeneration, Beijing Advanced Innovation Center for Biomedical Engineering, School of Biological Science and Medical Engineering, Beihang University, Beijing 100083, China

** Corresponding author.

*** Corresponding authors.

**** Corresponding author. Guangdong-Hongkong-Macau Institute of CNS Regeneration, Jinan University, Guangzhou, 510632, China.

E-mail addresses: hmaskf@hku.hk (K.-F. So), chenlianghs@126.com (L. Chen), maoying@fudan.edu.cn (Y. Mao), lxgchina@sina.com (X. Li).

¹ These authors contributed equally: Jiao Mu, Xiang Zou, Xinjie Bao, Zhaoyang Yang.

<https://doi.org/10.1016/j.bioactmat.2024.12.017>

Received 4 October 2024; Received in revised form 6 December 2024; Accepted 17 December 2024

2452-199X/. 2024 The Authors. Publishing services by Elsevier B.V. on behalf of KeAi Communications Co. Ltd. This is an open access article under the CC BY-NC-ND license (<http://creativecommons.org/licenses/by-nc-nd/4.0/>).

1. Introduction

Ischemic stroke causes substantial loss of neurons, resulting in irreversible neurological dysfunctions [1]. Previous studies have focused on the ischemic penumbra field surrounding the stroke cavity, and tried to protect residual neurons, axons, and vessels [2,3]. Recently, ultrasmall iron-gallic acid coordination polymer nanodots (Fe-GA CPNs) were developed as antioxidative neuroprotectors for ischemia stroke therapy guided by PET/MR imaging [4]. In addition, biomimetic nanoplateforms were reported to preventing neuroinflammation and scavenge excess reactive oxygen species in penumbra [5]. Although these advanced research are aimed at discovering promising strategies to limit neuronal or vascular damage in the penumbra, how to replace the damaged or dying neurons and vessels in the stroke cavity to treat ischemic stroke fundamentally remains unsolved.

In the adult mammal brain, neural stem cells (NSCs) reside within the subventricular zone (SVZ) in the lateral ventricles and the subgranular zone (SGZ) in hippocampus. NSCs act as “seeds” in the central nervous system, and can self-renew and generate new neurons and glia cells in adulthood [6–8]. Ischemic stroke induce the proliferation of NSCs in the SVZ, their migration from SVZ toward the penumbra, and their differentiation into new-born neurons [9]. Indeed, entering the stroke cavity to facilitate functional repair is difficult for new-born neurons because the stroke cavity reorganizes into a chamber wrapped by fibrotic scar and devoid of extracellular matrix and vascular nutrition over time. Therefore, the stroke cavity represents an ideal transplant location that can accept biomaterial injection without affecting the normal brain, which provides physical support for cell infiltration and exogenous molecules for the activation of angiogenesis and endogenous neurogenesis.

The biomaterial strategy delivers acellular biomaterials into the stroke cavity and slowly releases various regeneration-promoting factors to activate endogenous neurogenesis and angiogenesis [10]. Chitosan is a versatile biopolymer with biocompatibility, biodegradability, and mucoadhesiveness. Chitosan serves as a multifunctional scaffold facilitating the angiogenesis and regeneration of diverse tissues by promoting cell adhesion and proliferation [11,12]. In addition, chitosan have attractive biological activities, the antimicrobial, antioxidant, anticancer, anti-inflammatory activities [13,14]. Numerous chitosan-based biomaterials have been applied as vehicles for neurotrophic factors, stem cell, genetic material, or bioactive molecule delivery [15,16]. Basic fibroblast growth factor (bFGF) is known to promote angiogenesis, proliferation and migration of neural progenitor cells (NPCs) [17,18]. We successfully loaded bFGF onto chitosan gel, enabling its long-term controlled release bFGF for up to nine weeks [19]. The approach addresses limitation of soluble bFGF, including poor stability and short half-life. By directly administering the bFGF-Chitosan gel into the stroke cavity, it remains in the stroke cavity to perform its biological function, thereby mitigating the risks of infection and edema associated with continuous injection of soluble bFGF in clinical setting.

Previously, we have reported that bFGF-Chitosan gel effectively promotes differentiation of NSCs into functional neurons and establishes synaptic contacts in vitro [20]. The direct injection of bFGF-Chitosan gel into the ischemic stroke cavity in rat promoted angiogenesis and activated endogenous NSCs, guided NSCs to migrate into the stroke cavity and differentiate into mature neurons, and finally improved the sensorimotor functional recovery [19]. However, whether proliferated vessels integrated into the host vasculature and restored cerebral blood flow supply, whether new-born neurons formed functional synapses and reconstructed neural circuits, where new-born neurons were derived from, and whether new-born neurons and their synaptic connection participated in functional recovery after ischemic stroke remain unclear.

2. Materials and methods

2.1. Animals

All animals were approved (No. AEE-2022-225 and No. AEEI-2019-151) and monitored by the Animal Care Committee of Capital University of Medical. Yong C57BL/6 J mice (20–25 g, 8–12 weeks old) and Wistar rats (200–250 g, 8–12 weeks old) of both sexes were used. All transgenic mice were on a predominantly C57BL/6 J background, including B6. Cg-Gt(ROSA)26Sor^{tm14(CAG-tdTomato)Hze/J} (JAX #007914), B6.129P2-Gt(ROSA)26Sor^{tm1(DTA)Lky/J} (JAX #009669), C57BL/6-Tg(Nes-cre/ERT2)KEisc/J (JAX #016261). The animals were housed in sterile plastic cages (3–5 per cage) and had unlimited access to food and water. They were kept in a temperature-controlled (21–23 °C) room with a relative humidity of 50%–60 % and a 12 h (h) light/dark cycle.

Animals were randomized to groups, except when group allocation was genotype-dependent. Animals were divided into four groups: sham group (animals received no ischemic stroke), stroke alone group (animals received ischemic stroke, while no transplantation of gel), chitosan gel alone group (chitosan gel loaded without bFGF were injected into stroke cavity on day 7 after stroke), and bFGF-Chitosan gel group (chitosan gel loaded with bFGF were injected into stroke cavity on day 7 after stroke). Because the previous studies have demonstrated that the surgical procedure of removal of the necrotic tissues or single intraventricular injection of soluble bFGF do not promote endogenous neurogenesis [19,20], lesion control group and soluble bFGF group were not set in our study. The experiments and analyses were conducted blinded to group allocation. Sample sizes were determined based on previous work using similar methods [21]. The number of animals used in each part of the study was summarized in Tables S1–S5.

2.2. Preparation of bFGF-Chitosan gel

bFGF-Chitosan gel was prepared as described previously [20]. Briefly, Ten-milligram deacetylated chitosan particles (Sigma, USA) were swollen in 10 mL deionized water for 6 h, and the upper liquid was discarded after centrifugation. The swollen chitosan particles were frozen at – 20 °C for 24 h and then stood at 4 °C for 10 h. Twenty nanograms of bFGF (Yisheng, China) was dissolved in 1 mL cold deionized water and stirred with chitosan particles at 4 °C for 6 h and dried in vacuum. Finally, the mixture was added to a collagen I solution and stirred at 4 °C for 30 min. bFGF-Chitosan was collected after centrifugation and stored at 4 °C.

2.3. Establishment of cortical photothrombotic stroke model and implantation of gel

In our previous study, a detailed surgical process of photothrombotic stroke in mice has been described [22]. Briefly, mice was intraperitoneally injected with 1 % pentobarbital sodium (50 mg/kg, Cat# Tc-P8411, Merck, Darmstadt, Germany), and the head was immobilized in a stereotactic apparatus. A window was drilled into the skull above the forelimb area of the right motor cortex at the following coordinates relative to the bregma: anterior-posterior (AP): –0.5mm to +1 mm, medial-lateral (ML): –0.75mm to –2.25 mm. Rose Bengal solution (10mg/ml, 8 mL/kg) was administered by tail vein injection. Then, the cortex in skull window was illuminated for 2min by a 532-nm fixed wavelength laser (GPD105-M-12, Taiwan Shuanzhou Photoelectric Co., Ltd., Taiwan, China) creating a 1.5-mm diameter illumination spot with positioned 1.0 cm from the skull window. The above procedure was for mice in the stroke alone group. In the sham group, mice underwent the same surgical procedure without illumination.

Meanwhile, photothrombotic stroke model in rats was established as our previous study [19]. Briefly, the rat was intraperitoneally injected with 1 % pentobarbital sodium (50 mg/kg, Cat# Tc-P8411, Merck, Darmstadt, Germany), and the head was immobilized in a stereotactic

apparatus. A window was drilled into the skull above the forelimb area of the right motor cortex at the following coordinates relative to the bregma: AP: -0.5 mm to $+1.5$ mm, ML: -1.5 mm to -3.5 mm. The dura mater was kept intact. Rose Bengal solution (40 mg/ml, 80 mg/kg) was administered by femoral vein injection. Then, the cortex in skull window was illuminated for 10 min by a 532-nm fixed wavelength laser (GPD105-M-12, Taiwan Shuanzhou Photoelectric Co., Ltd., Taiwan, China) creating a 2.0-mm diameter illumination spot with positioned 1.0 cm from the skull window. The above procedure was for rats in the stroke alone group. In the sham group, rats underwent the same surgical procedure without illumination.

A detailed surgical process for gel transplantation has been reported in our previous studies [19]. On day 7 post-stroke, the necrotic tissue in the stroke cavity was removed using an in-house biological tissue suction device (ZL 20191 1140256.1). Subsequently, chitosan gel load with or without bFGF were immediately transplanted into the stroke cavity (0.15 mg in mice and 0.2 mg in rat). The dura mater, muscles, and skin were then sutured, and the wound was sterilized. Penicillin (2 units/100 g, intraperitoneal injection) was administered daily for 7 days to minimize inflammation.

2.4. BrdU administration

To trace the fate of proliferated cells, BrdU was intraperitoneally injected (50 mg/kg in 0.9 % NaCl, Sigma-Aldrich) to the animals once every 12 h for 5 days, commencing 24 h after photothrombotic surgery and biomaterials implantation, respectively.

2.5. Blood flow imaging

Cerebral blood flow (CBF) was imaged by a high-resolution Laser Speckle Contrast Imager (LSCI, Pericam PSI, Perimed Inc., Sweden) on day 60 post-ischemic stroke. Mice was anesthetized and restrained in a stereotaxic frame to minimize the influence of breathing motion on the head. The scalp was gently incised, and the skull was exposed to capture the recordings. The camera of the imager was adjusted to 20 cm for all perfusion recordings. CBF in the ipsilateral (ischemic) motor cortex (1 mm radius from central point of the stroke cavity) and the contralateral (non-ischemic) motor cortex was selected and analyzed. The relative cerebral blood (rCBF) was calculated by dividing the ipsilateral CBF of ischemic cortex by the contralateral CBF of normal cortex [23].

2.6. Virus injection to reveal neural circuit reconstruction

To investigate the ability of new-born neurons in the stroke cavity to receive long-distance projections from contralateral cortex, an anterograde tracing virus, AAV2/9-hSyn-mCherry (8.2×10^{12} vg/ml) (BrainVTA Technology Co., Ltd), was injected into contralateral motor cortex on day 56 post-ischemic stroke. Briefly, 150 nL of virus was injected into three different points in the contralateral motor cortex at a rate of 50 nL/min: AP $+0.8$ mm, ML -1.8 mm, dorsal-ventral (DV) -0.5 mm; AP $+0.4$ mm, ML -1.2 mm, DV -0.5 mm; and AP $+0.2$ mm, ML -1.5 mm, DV -0.5 mm. The pipette was left in place for an additional 3 minutes after the final injection at each site before slowly removed. Mice was sacrificed 3 weeks after injection to study the expression of new-born neurons and mCherry-positive fibers in the stroke cavity [24].

2.7. Relationship between synaptogenesis and recovery of behavioral disorders

To investigate the relationship between synaptogenesis in stroke cavity and recovery of behavioral disorders, behavior analyses were conducted prior to stroke and on day 3, and day 35 post-stroke. Subsequently, on day 42 post-stroke, rAAV-hSyn-TeLC-P2A-mCherry (2.0×10^{12} vg/ml) (BrainVTA Technology Co., Ltd) was injected into the stroke cavity to disrupt synaptic transmission. As control, an equivalent

volume of negative control rAAV-hSyn-mCherry (2.0×10^{12} vg/ml) (BrainVTA Technology Co., Ltd) was used. Briefly, 150 nL of virus was injected into three different points in the contralateral motor cortex at a rate of 50 nL/min: AP: $+1$ mm, ML: -1.25 mm, DV: -0.6 mm; A/P: 0 mm, ML: -1 mm, DV: -0.6 mm; AP: 0 mm, ML: -2 mm, DV: -0.6 mm. After the final injection at each site, the pipette was left in place for additional 3 minutes before slowly removed. Behavior tests were conducted 3 weeks post-injection.

2.8. Immunohistochemistry

After anesthetized, animals were perfused transcardially with 20 mL 0.9 % saline followed by 4 % PFA. The brains were then post-fixed by immersion overnight and then to undertake dehydration with 30 % sucrose for three days. Using a freezing microtome, the brain tissues were sliced into 30- μ m-thick sections. A total of 30 brain slice were randomly divided for 10 sets for immunohistochemistry following our previous study [20]. For immunofluorescence staining, the brain sections stained for BrdU were first denatured with 2 N HCl at 37 °C for 25 min and then renatured with 0.1 M sodium tetraborate (pH 8.4) at 37 °C for 10 min. The primary antibodies and dilutions were as follows: rat anti-BrdU (1:200, ab6326, Abcam), rabbit anti-GluT1 (1:500, ab115730, Abcam), rabbit anti-DCX (1:500, ab18723, Abcam), rabbit anti-Tuj1 (1:500, T2200-200UL, T2200, Sigma-Aldrich), rabbit anti-NeuN (1:500, ab177487, Abcam), mouse anti-BrdU (ZM-0013, ZSGB-BIO), rabbit anti-SV2A (1:200, ab273513, Abcam), rabbit anti-SynapsinI (1:200, 5297S, Cell Signaling Technology), rabbit anti-PSD95 (1:200, 3450S, Cell Signaling Technology), rabbit anti-Sox2 (1:200, 43360S, Cell Signaling Technology), rabbit anti-CD133 (1:200, ab19898, Abcam), rabbit anti-MASH1 (1:200, ab74065, Abcam), rabbit anti-Nestin (1:100, ABD69, Millipore), rat anti-NeuN (1:500, ab279297, Abcam), rabbit anti-SATB2 (1:200, ab92446, Abcam), rabbit anti-CTIP2 (1:100, ab240636, Abcam), rabbit anti-CamKII α (1:200, ab52476, Abcam), rabbit anti-GABA (1:400, NBP2-43558, NOVUS), rabbit anti-IBA1 (1:500, ab178847, Abcam), rabbit anti-GFAP (1:500, ab4674, Abcam), rat anti-Ki67 (1:300, 14-5698-82, Invitrogen), rat anti-mCherry (1:500, ARG10760, Arigo). The secondary antibodies were: Alexa Fluor-488/594-conjugated goat anti-rabbit IgG, Alexa Fluor-405-conjugated goat anti-mouse IgG, and Alexa Fluor-488/647-conjugated-goat anti-rat IgG (all 1:200, Jackson ImmunoResearch Laboratories, Inc., West Grove, PA, USA) respectively. Cell nuclei were counterstained with Hoechst 33258 (1:1000, 94403, Sigma-Aldrich) or Topro (1:1000, T3605, Invitrogen) for 8 min before being mounted with a coverslip and mounting medium.

A detailed process of immunohistochemical staining has been described in our previous study [25]. Briefly, brain sections were washed three times with 0.01 M PBS and the endogenous peroxidase were blocked using 3 % H₂O₂ for 30 min. Then, the sections were incubated with goat serum to reduce non-specific reaction for 60 min, following the incubation with the bFGF primary antibody (rabbit anti-FGF2, 1:50, 11234-1-AP, Proteintech) at 4 °C overnight. After washing with 0.01 M PBS, biotinylated goat anti-rabbit secondary antibody and S-A/HRP reagent were applied subsequently at room temperature for 6 hours, respectively. The positive reaction was visualized with DAB, and the section was then dehydrated in graded alcohols, cleared in xylene and covered.

2.9. Motor evoked potentials (MEPs)

MEP measurements were conducted using Nicolet CR Endeavor (Nicolet, Madison, USA) on day 60 after ischemic stroke. After anesthesia, mice were restrained in a stereotaxic frame. The scalp was gently incised, and the skull window was re-exposed. MEPs were recorded using subdermal needle electrodes (stainless steel, Viasys, 698–621700) placed on the left biceps brachii. Stimuli were delivered via stimulating electrodes targeting the cortex in the stroke cavity. The stimuli

comprised five consecutive train at a frequency of 350 Hz, with a maximum stimulus intensity of 2 mA. For the sham mice, stimuli were applied using corkscrew electrodes targeting the cortex at the same position as stroke cavity [26,27].

2.10. PET/CT

To examine the synaptic density *in vivo* post-stroke, PET/CT experiments were performed using a Siemens Inveon PET/CT system (Siemens Medical Solutions, Knoxville, United States) on day 63 after ischemic stroke. The [¹⁸F] SDM-8 tracer was produced as previously described [28,29]. The rats were anesthetized using an isoflurane vaporizer (Molecular Imaging Products Company, USA). Subsequently, [¹⁸F] SDM-8 tracer was administered by tail vein injection (0.2–0.5 mL, 0.37 MBq/g body weight). After 60 min, the rat was positioned prone in a plastic stereotaxic frame designed to fit in the gantry of the micro-PET/CT and imaged for 30 min, while a T1-weighted MR scan was simultaneously acquired. PET/CT images were reconstructed using the ordered subsets expectation maximization 3D algorithm (OSEM3D). The measurements were performed using Inveon Research Workplace (IRW) software (Siemens). The outcome measure was standardized uptake value (SUV) in each brain region. The SUV ratio (SUV_R) was calculated as the ischemic motor cortex SUV value divided by the medulla SUV value [29].

2.11. Immuno-electron microscopy

On day 63 post-stroke, rats were sacrificed for immune-gold labeling as previously reported [21]. Briefly, animals were perfused transcardially with 20 mL 0.9 % saline, followed by a mixture of 2 % glutaric dialdehyde and 4 % PFA. Subsequently, the brains underwent post-fixation with 4 % PFA for 6 h, then were sectioned using oscillating microtome to provide 60-nm-thick tissue slices for immune-electron staining. Five sections per rat were randomly selected and washed with 0.01 M PBS. Then these brain sections were incubated with 10 mg/ml sodium borohydride for 10min, 3 % H₂O₂ for another 10min, 10 % NGC for 1h, and overnight with primary antibody rabbit anti-MAP2 (1:200, AB5622, Millipore) at 4°C. The brain sections were incubated with goat anti-rabbit secondary antibody bound with 0.4 nm nanogold (1:50) for 2 h at room temperature, then fixed by 2 % glutaric dialdehyde for 1 h. The gold particles were enhanced using a HQ SILVER kit (Nanoprobes, Inc) for 8 min. The sections were subsequently post-fixed in 2 % osmium tetroxide, dehydrated in alcohol and acetone, and then flat-embedded in epoxy resin. The samples were finally cut into 70-nm-thick sections, stained with uranyl acetate and bismuth subnitrate, and examined under a transmission electron microscope (JEOL, Peabody, MA, USA).

2.12. MED64 planar multielectrode array system recording

To determine whether bFGF-Chitosan gel induced new-born neurons in the stroke cavity integrate into the adjacent region of host brain, electrophysiology was recorded on day 63 after ischemic stroke using MED64 Planar Multielectrode Array recording system (MED64, Alpha MED Scientific Inc., Japan), as reported previously [30]. Briefly, rats were anesthetized and perfused transcardially with ice-cold dissection solution comprising (g/L): glucose 1.8016, sucrose 72.9078, NaHCO₃ 2.1843, KCl 0.2237, NaH₂PO₄·H₂O 0.138, CaCl₂·2H₂O 0.0735, MgCl₂·6H₂O 1.0165, PH 7.2–7.4. The brain was promptly extracted and sliced into longitudinal sections of 350µm thickness. These sections were incubated at 34 °C for 60 min, continuously bubbled with 95 % O₂ and 5 % CO₂ in the artificial cerebrospinal fluid containing (g/L): NaCl 7.305, glucose 1.8016, NaHCO₃ 2.1843, KCl 0.3728, NaH₂PO₄·H₂O 0.1655, CaCl₂·2H₂O 0.3822, MgCl₂·6H₂O 0.2643. Then, a brain slice was transferred to an 8 × 8 array of the planar microelectrode (MED-P515, Alpha MED Sciences, Osaka, Japan), each electrode being 50 × 50µm,

with a space of 300µm. Field excitatory postsynaptic potentials (fEPSPs) were recorded in the stroke cavity by selecting an electrode in the host brain as the stimulating electrode. After a stable baseline of 30 min, drugs were administered respectively in the following: tetrodotoxin (TTX, 0.5 µM, Sigma-Aldrich), and 6-cyano-7-nitroquinoxaline-2,3-dione (CNQX, 10 µM, Sigma-Aldrich). Following inhibition of fEPSPs amplitude, the slice was perfused with oxygenated CSF until the drug effects disappeared and the normal fEPSPs recovered.

2.13. Morphological assessment

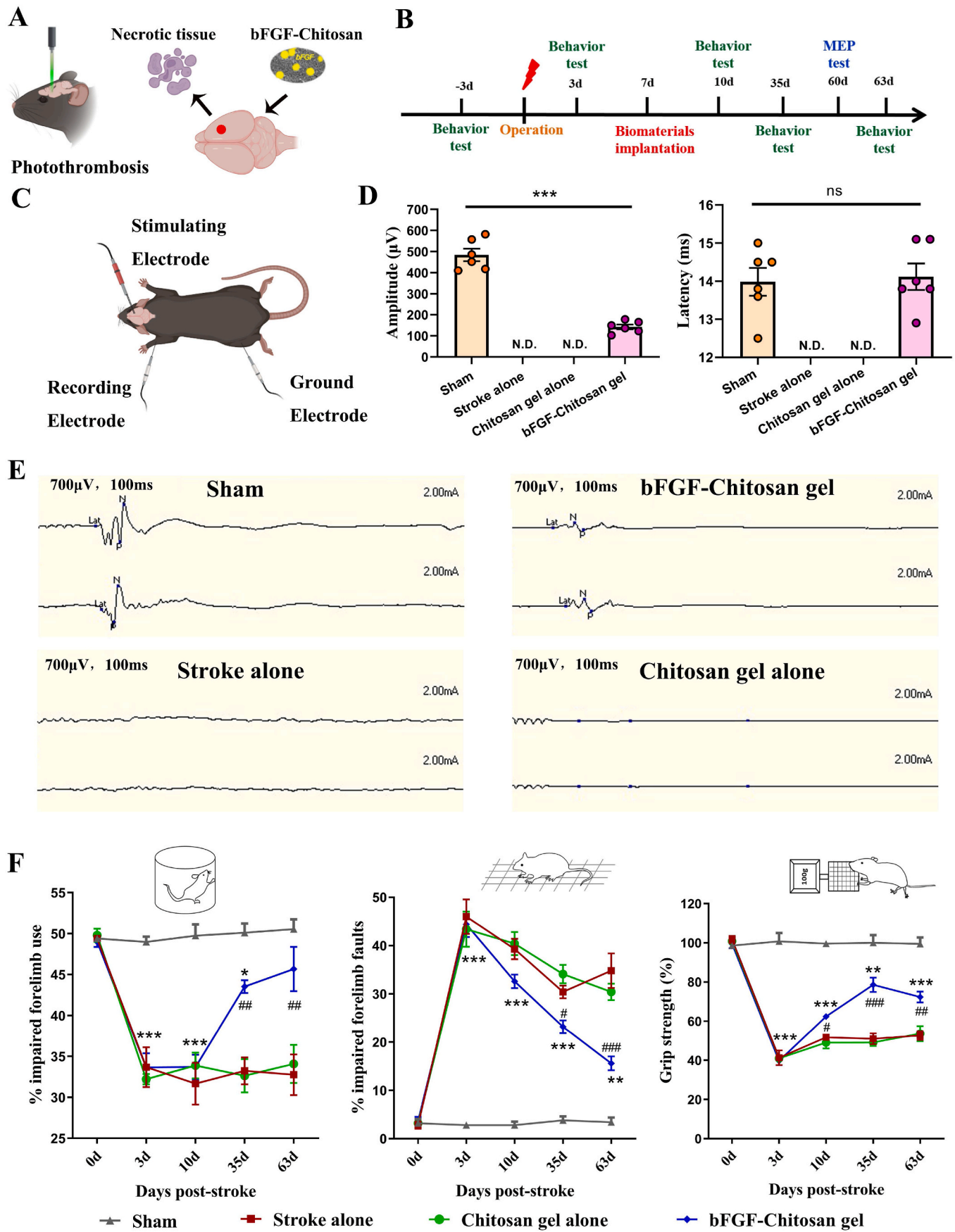
The sections underwent a thorough examination using a confocal microscope (TCS SP8, Leica, Germany) or a Panoramic SCAN slide scanner (3D Histech). A quantitative analysis was conducted on the microscopic images captured through imaging. A detailed assessment of cell counts and positive fluorescent areas were performed at a magnification of 630 × for each section. The regions of interests (ROIs) for quantification of GluT1, Tuj1, and NeuN positive cells were measured within the stroke cavity. The ROIs for IBA1, DCX, CD133, Sox2, and MASH1 positive cells were measured in peri-infarct cortex [31]. ImageJ software was used for image measurement and analysis. To determine the area fraction, the images were binarized, and the Analyze Particles tool was utilized to determine area fraction. For assessing fluorescence intensity, the regions of interest were outlined with a selection tool and the measure function was used to determine intensity. In terms of vascular diameter, vessel boundaries were outlined using the line selection tool to measure vascular diameter [22]. Cell density was determined by calculating the number of cells/frame area (25 µm × 25 µm) [21]. The microglia morphological analysis: high-resolution images of microglia were acquired using a confocal microscope at 0.5µm intervals. Reconstruction of microglia was carried out using Imaris software [32]. Then Sholl plugin of ImageJ software was used to analyze the number of dendrites that cross concentric circles at increasing distances from the soma (1.5µm interval) [33].

2.14. Behavioral testing

To assess forelimb sensorimotor function recovery after stroke, behavior analyses were conducted, including cylinder experiment, grid walking test, and grip strength test. These tests were performed before photothrombotic surgery and on day 3, day10, day 35 and day 63 post-surgery. The cylinder test was utilized to examine forelimb use asymmetry during vertical exploration [19]. Mice was placed in a transparent, round glass cylinder (10 cm diameter 15 cm tall). Typically, mice rear up to an upright position and use one or both forelimbs for support against the cylinder wall. Mice was record for at least 3 minutes. Videos were later rated offline. The percentage of impaired forelimb use was calculated as follows: % (impaired forelimb use + ½ both forelimb use)/total forelimb use [19].

The grid walking test was used to assess motor function for accurate limb placement associated with plantar sensory feedback [34]. Mice was placed on an elevated wire grid and allowed to move freely. Faults were defined as steps where the paw missed the wire grid, slipped, or when the wrist or forearm, rather than the paw, were used for support. Mice was record for at least 3 minutes, and videos were rated offline. Stepping faults in the impaired forelimb were counted relative to the total 50 steps [34].

The grip strength test was used to assess muscle strength and coordination [20]. The peak force (g) produced by the impaired forepaw to resist a pulling force was tested by gently pulling the mouse's tail backward when the impaired forepaw grasped the sensor metal grid. Each was evaluated three times at each time point, and the grip strength of impaired forepaw was recorded [20].



(caption on next page)

Fig. 1. bFGF-Chitosan gel promotes recovery of sensorimotor function after ischemic stroke.

(A) Schematic diagram of the photothrombotic model and gel implantation. (B) Timeline of experimental procedure for functional test in C57BL/6J mice. MEP, Motor evoked potentials. (C) Schematic diagram of the MEP test. (D) Quantification of MEP amplitude and latency on day 60 post-stroke. *** $P < 0.001$, ns, no significant difference, independent-samples T test, $n = 6$ in each group. (E) Representative MEP signal in each group. (F) bFGF-Chitosan gel promotes recovery of sensorimotor function. * $P < 0.05$, ** $P < 0.01$, *** $P < 0.001$, bFGF-Chitosan gel group compared with the sham group. # $P < 0.05$, ## $P < 0.01$, ### $P < 0.001$, bFGF-Chitosan gel group compared with the stroke alone group, two-way ANOVA, $n = 5$ in each group. Data are presented as mean \pm SEM. Schematic diagram was created with BioRender.com.

2.15. Tamoxifen induction

Mouse DNA was extracted for PCR reactions, and positive mice were selected for backup after DNA gel electrophoresis and imaging. When the mice was eight weeks old, tamoxifen was intraperitoneally injected (0.2 mL/10g in corn oil solution) once a day for 4 days before photothrombotic surgery to induce the expression of Cre recombinant enzyme-dependent fusion protein. Following the injection cycle, tamoxifen was cleared for 7 days, and then photothrombotic surgery was conducted [35].

2.16. Electrophysiology

On day 63 post-stroke, the mice was anesthetized and placed back on the stereotaxic frame. Once the skull was exposed, two small holes were drilled in the skull to allow the electrodes implantation in the brain. A bipolar silver stimulating electrode was placed into the left motor cortex (AP +0.5mm, ML +1.5mm, DV -0.5mm). A concentric recording electrode was placed into the right motor cortex (AP +0.5mm, ML -1.5mm, DV -0.5mm). The ground electrodes was placed over the right hemispheres of the cerebellum. The test stimuli were delivered to the left motor cortex (bipolar pulses, 100- μ s duration each pulse, 60-s inter-pulse interval, 1/60 Hz, 0.7mA), while recording field postsynaptic potentials (fPSPs) from the stroke cavity. For the sham mice, concentric recording electrode was placed into the right motor cortex at the same position as stroke cavity.

2.17. Statistical analysis

Data were presented as mean \pm SEM. Measurements from individual animals were shown on plots plotted as datapoints wherever possible. SPSS23.0 and Prism 8.0 (GraphPad Prism Software) were used for statistical analyses and graphing of quantitative data. The One-Sample Kolmogorov-Smirnov Test was used for data normality analysis, while Levene's test was used to test for homogeneity of variance. Two independent samples were compared using the independent-samples T-test. Multiple statistical analysis comparisons were performed by one-way analysis of variance (ANOVA). Bonferroni post hoc test was used to assess data variance, and Dunnett's T3 post hoc test for data of unequal variance. Two-way ANOVA were utilized for behavioral statistical analyses and Sholl analyses. Details on the statistical tests used for each experiment are provided in the results and figure legends. $P < 0.05$ was considered statistically significant.

3. Results

3.1. bFGF-Chitosan gel promotes the recovery of sensorimotor function after ischemic stroke

The cortical ischemic model was established by photothrombosis, where focal infarction is restricted to the right forelimb representation of the sensorimotor cortex [22]. On day 7 post-stroke, most of the neurons [22] and vessels (Fig. S1) in the stroke cavity had disintegrated, and formed a stable stroke cavity. The number of proliferated neuroblasts in the SVZ peaked in quantity (Fig. S2), while the microglia-mediated inflammatory response and astrocyte-formed glia scar had not yet reached their peak (Fig. S3), which is consistent with the previous study [36,37]. Therefore, day 7 post-stroke was selected as the optimal intervention

time point to transplant the chitosan gel load with or without bFGF into the stroke cavity (Fig. 1A). The implantation of bFGF-Chitosan gel significantly increased the expression of bFGF in the stroke cavity and diffused bFGF within 300 μ m distant from the infarct on day 14 post-stroke (Fig. S4).

To assess the changes in motor conduction function from the motor cortex to the target muscle of contralateral forelimb under different interventions, motor evoked potentials (MEPs) were recorded on day 60 post-ischemic stroke (Fig. 1B and C). In the sham group, MEPs were recorded by subdermal needle electrodes from the left bicep brachii when stimuli were applied to the right sensorimotor cortex, whereas no MEPs was recorded when stimuli were applied to the stroke cavity in stroke alone group and chitosan gel alone group. Conversely, motor responses were elicited in the bFGF-Chitosan gel group when stimuli were applied to the stroke cavity. Compared with the sham group (484.23 \pm 29.29 μ V), the MEP amplitude decreased to 142.60 \pm 11.25 μ V ($P < 0.001$) in the bFGF-Chitosan gel group, whereas the MEP latency did not change significantly (sham group 13.98 \pm 0.36 ms vs. bFGF-Chitosan gel group 14.12 \pm 0.35 ms, $P > 0.05$) (Fig. 1D and E). These results indicated that bFGF-Chitosan gel improved motor conduction function in mice after ischemic stroke.

Next, behavior analyses, including cylinder experiment, grid walking test, and grip strength test, were conducted to evaluate the recovery of forelimb sensorimotor function after stroke. In the sham mice, the usage rate of the right forelimb was approximately 50 %, and the misstep rate was only about 3 %. On day 3 post-stroke, the usage rate of the impaired forelimb was decreased to about 30 %, the misstep rate was increased to about 45 %, and the grip strength dropped to about 40 % of baseline, indicating ischemic stroke impaired sensorimotor function in the contralateral forelimb. Although the mice in the stroke alone group and the chitosan gel alone group displayed spontaneous recovery, it was far from achieving the normal baseline levels at 2 months after stroke. In the bFGF-Chitosan gel group, the mice showed significant sensorimotor functional improvement from day 35 post-stroke (bFGF-Chitosan gel group vs. stroke alone group: cylinder experiment 43.54 \pm 0.78 vs. 33.24 \pm 1.66, $P < 0.01$; grid walking test 23.20 \pm 1.36 vs. 30.40 \pm 1.33, $P < 0.05$; grip strength test 78.55 \pm 3.65 vs. 50.99 \pm 2.75, $P < 0.001$). Moreover, the usage rate of the impaired forelimb in the bFGF-Chitosan gel group was near normal baseline levels on day 63 post-stroke (bFGF-Chitosan gel group vs. sham group: cylinder experiment 45.68 \pm 2.70 vs. 50.55 \pm 1.20, $P > 0.05$; grid walking test 15.60 \pm 1.47 vs. 3.40 \pm 0.98, $P < 0.01$; grip strength test 72.37 \pm 2.80 vs. 99.41 \pm 3.25, $P < 0.001$), as shown in Fig. 1F. These results suggested that bFGF-Chitosan gel promoted long-term recovery of sensorimotor function in mice after ischemic stroke.

3.2. bFGF-Chitosan gel enhances angiogenesis, reconstructs vascular network, and restores cerebral blood flow in and about stroke cavity

Previous studies have proved that neurogenesis and angiogenesis are coupled processes after ischemic stroke, which are critical in improving post-stroke neurological functional recovery [38]. To investigate the extent of tissue neovascularization under different interventions, BrdU was intraperitoneally injected for five consecutive days after photothrombotic surgery and chitosan gel implantation, respectively. We prepared coronal brain sections and performed BrdU/GluT1 (a marker for vascular endothelial cell) immunofluorescence staining to detect proliferated endothelial cells on day 63 post-stroke (Fig. 2A and B). In

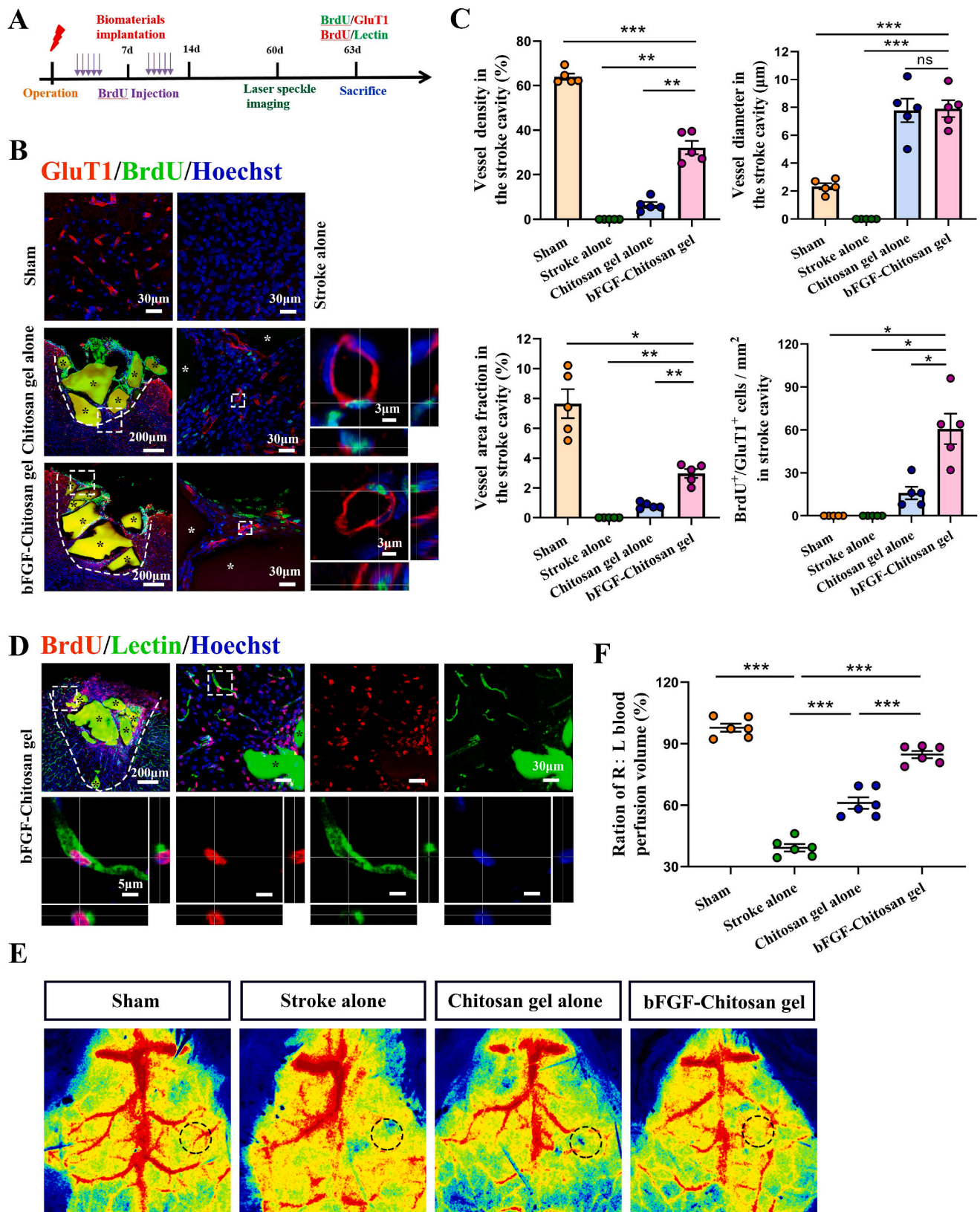
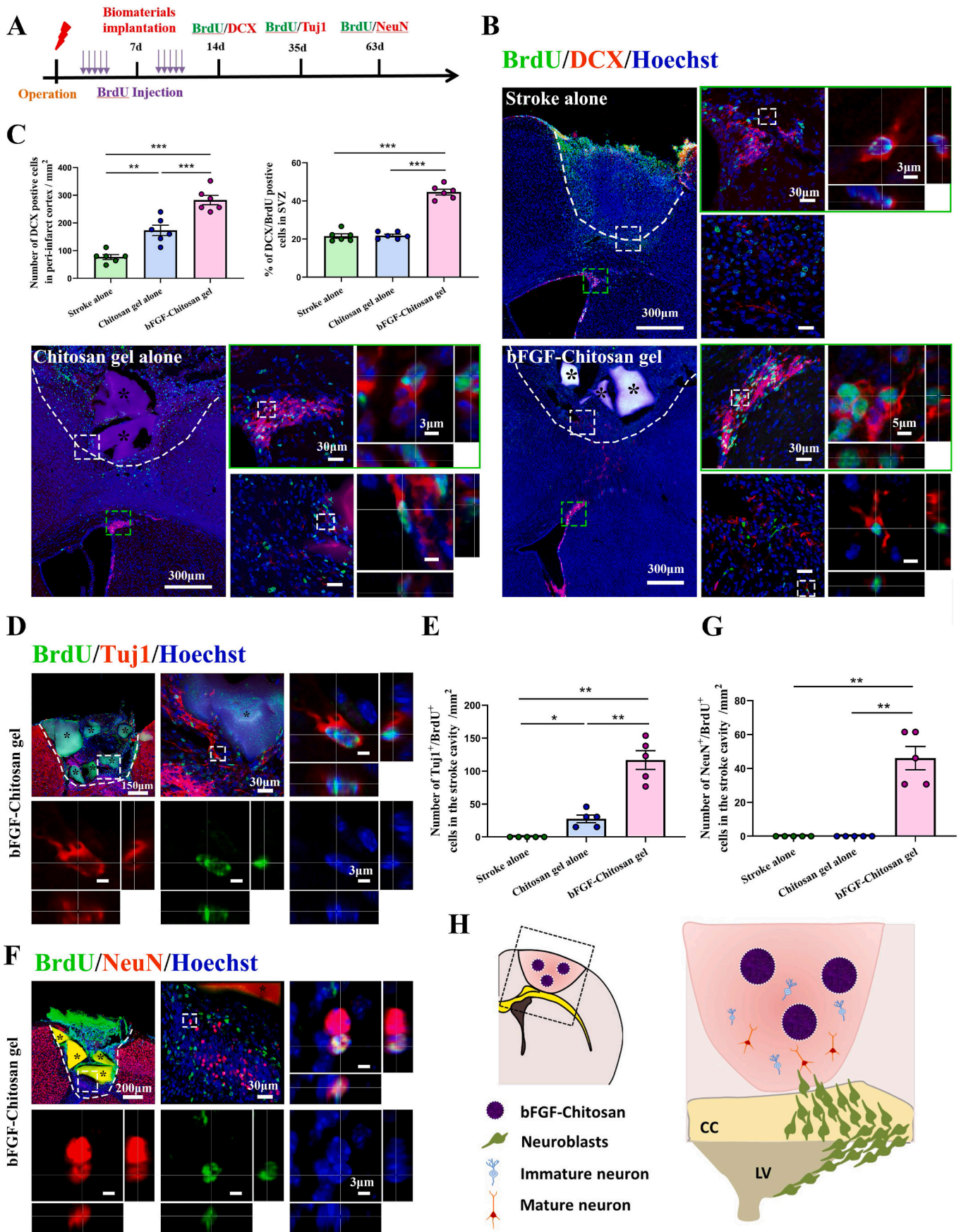


Fig. 2. bFGF-Chitosan gel enhances angiogenesis, revascularization and restoration of cerebral blood flow in and about stroke cavity. (A) Timeline of experimental procedure for angiogenesis examination. (B) Representative immunofluorescence images of new-born vascular endothelial cells in and around stroke cavity (GluT1/BrdU/Hoechst) on day 63 post-stroke. (C) Quantification of vessel area fraction, vessel density, vessel diameter and cell density of BrdU/GluT1 in stroke cavity on day 63 post-stroke. * $P < 0.05$, ** $P < 0.01$, *** $P < 0.001$, ns, no significant difference, one-way ANOVA and post-hoc Dunnett's T3 test, $n = 5$. (D) Representative immunofluorescence images of new-born functional vessel in the stroke cavity of bFGF-Chitosan gel mice (Lectin/BrdU/Hoechst) on day 63 post-stroke. (E) Representative blood flow maps on day 60 post-stroke. (F) Quantification of cerebral blood flow in and around the stroke cavity in each group on day 60 post-stroke. *** $P < 0.001$ one-way ANOVA and post-hoc Bonferroni tests. $n = 6$ in each group. Data are presented as mean ± SEM.



(caption on next page)

Fig. 3. bFGF-Chitosan gel facilitates production and long-term survival of new-born neurons in stroke cavity.

(A) Timeline of experimental procedure for neurogenesis examination. (B) bFGF-Chitosan gel promotes ectopic migration of neuroblasts toward the peri-infarct cortical region (white box) and increases neuroblast production in the SVZ (green box) on day 14 post-stroke. (C) Quantification of the number of neuroblasts in the peri-infarct cortical region and percentage of proliferated neuroblast in SVZ on day 14 post-stroke. $**P < 0.01$, $***P < 0.001$, one-way ANOVA and post-hoc Bonferroni tests. $n = 6$ in each group. (D) Representative immunofluorescence images of new-born immature neurons in the stroke cavity on day 35 post-stroke (Tuj1/BrdU/Hoechst). (E) Quantification of new-born immature neurons in the stroke cavity on day 35 post-stroke. $*P < 0.05$, $**P < 0.01$, one-way ANOVA and post-hoc Dunnett's T3 test. $n = 5$ in each group. (F) Representative immunofluorescence images of new-born mature neurons in the stroke cavity (NeuN/BrdU/Hoechst) on day 63 post-stroke. (G) Quantification of new-born mature neurons in the stroke cavity on day 63 post-stroke. $**P < 0.01$, one-way ANOVA and post-hoc Dunnett's T3 test. $n = 5$ in each group. Data are presented as mean \pm SEM. (H) Schematic diagram of the neuroblasts migrating from the SVZ toward the stroke cavity and differentiated into mature neurons. Schematic diagram was created with BioRender.com.

the stroke alone group, BrdU⁺/GluT1⁺ new-born endothelial cells were only detected in the peri-infarct cortical region, but not in the stroke cavity. The implantation of chitosan gel alone produced sparse BrdU⁺/GluT1⁺ new-born endothelial cells in the stroke cavity. By contrast, abundant BrdU⁺/GluT1⁺ new-born endothelial cells were detected in the stroke cavity of the bFGF-Chitosan gel group. Compared with the stroke alone group, mice in the bFGF-Chitosan gel group displayed a significantly increased vascular diameter, vessel area fraction, and vessel density in the stroke cavity (Fig. 2C). These results indicated that bFGF-Chitosan enhanced neovascularization in the stroke cavity.

Lectins can bind to the endothelial glycocalyx through direct injection into the blood circulation, thus they are widely used to label functional cerebral blood vessels [39,40]. To further investigate whether new-born vessel induced by bFGF-Chitosan gel in the stroke cavity develop into functional vascular networks, mice were administrated with fluorophore-conjugated lectin by tail vein injection 30 min before transcatheter perfusion on day 63 post-stroke. We prepared coronal brain sections and performed BrdU/Lectin immunofluorescence staining to label new-born functional vessel. The BrdU⁺/lectin⁺ functional new-born vessels were observed in the stroke cavity of the bFGF-Chitosan gel group (Fig. 2D). These results indicated that bFGF-Chitosan gel promoted the integration of new-born functional vessels into the host vasculature.

To further assess whether neovascularization facilitates the restoration of blood flow, we used laser speckle imaging to evaluate blood flow in and around the stroke cavity on day 60 post-stroke (Fig. 2E). Stroke caused a reduction blood flow in the stroke cavity to about 39 % of the sham group. The blood flow in the chitosan gel alone group decreased to about 61 % of sham group. By contrast, mice with bFGF-Chitosan gel implantation significantly increased blood flow to about 85 % of the sham group (Fig. 2F). Overall, our findings supported that bFGF-Chitosan gel promoted angiogenesis, revascularization, and restoration of cerebral blood flow supply in and around the stroke cavity.

3.3. bFGF-Chitosan gel facilitates production and long-term survival of new-born neurons in stroke cavity

To evaluate the effect of bFGF-Chitosan gel on proliferation and migration of neuroblasts after ischemic stroke, we prepared coronal brain sections and performed immunofluorescence staining to label DCX (a marker for neuroblasts) on day 14 post-stroke (Fig. 3A). Stroke induced DCX⁺ neuroblasts to migrate into the peri-infarct cortical region, while BrdU⁺/DCX⁺ proliferated neuroblasts were restricted to the SVZ. Compared with the stroke alone group, the implantation of chitosan gel alone produced a small but significant increase in the number of DCX⁺ neuroblasts in the peri-infarct region (chitosan gel alone group 173.33 ± 18.67 vs. stroke alone group 77.33 ± 8.68 mm², $P < 0.01$). By contrast, many more neuroblasts were distributed in the peri-infarct region in the bFGF-Chitosan gel group (bFGF-Chitosan gel group 282 ± 16.87 vs. stroke alone group 77.33 ± 8.68 mm², $P < 0.001$). In addition, the proportion of BrdU⁺/DCX⁺ proliferated neuroblasts and the density of Ki67⁺/DCX⁺ proliferating neuroblasts in the SVZ were significantly higher in the bFGF-Chitosan gel group compared with that in the stroke alone or chitosan alone groups (Fig. 3B–C and Figs. S5A–C). These results indicated that appropriately implanted bFGF-Chitosan gel

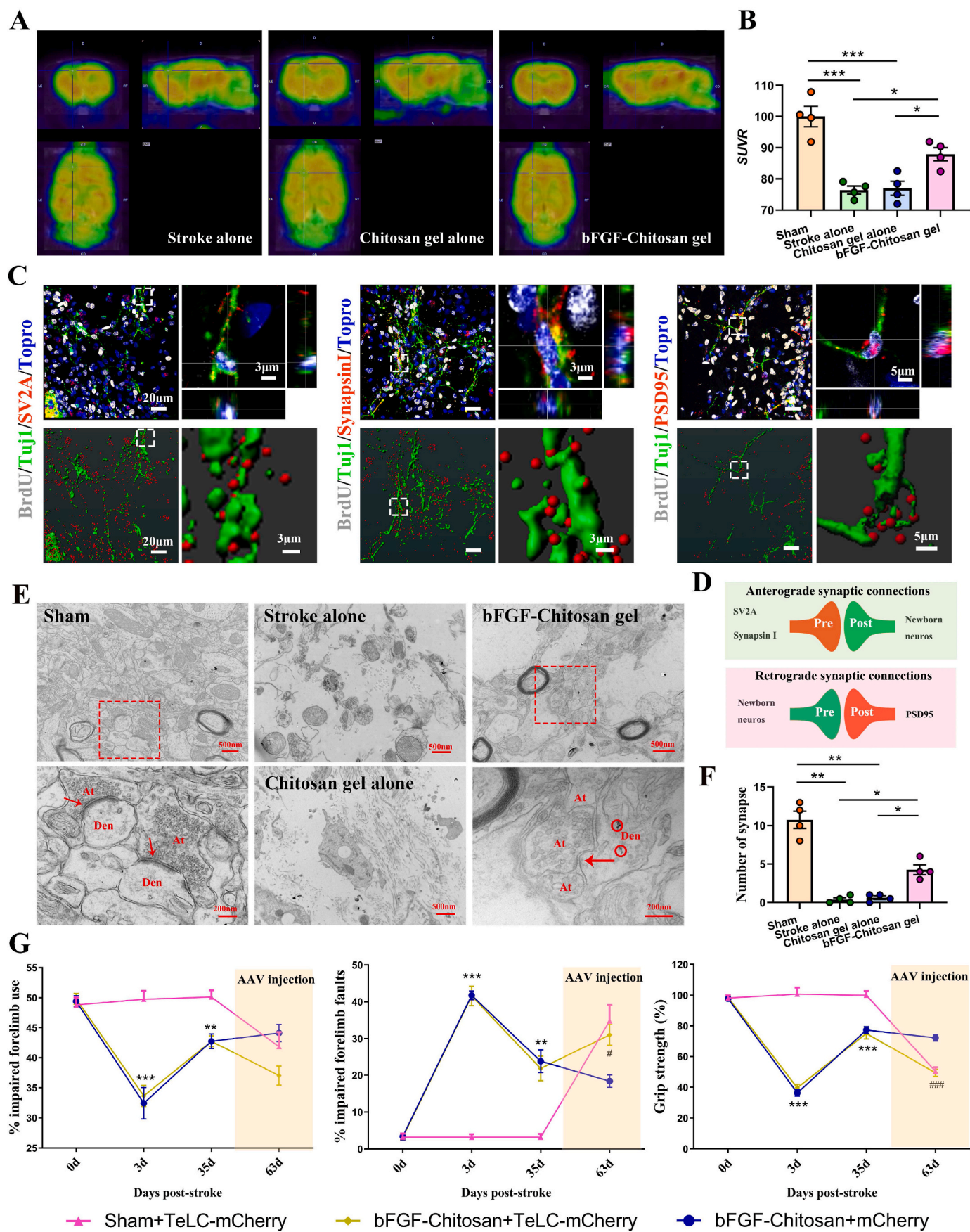
can promote the ectopic migration of neuroblasts to the peri-infarct cortical region while increasing the number of active neuroblasts in the SVZ.

To assess whether neuroblasts could differentiate into neurons, we prepared the coronal brain sections and performed immunofluorescence staining to label BrdU and Tuj1 (a marker for immature neurons) on day 35 post-stroke. In the stroke alone group, no Tuj1⁺ immature neurons were detected in the stroke cavity (Fig. S5D). Conversely, BrdU⁺/Tuj1⁺ new-born immature neurons in the stroke cavity were sparse in the chitosan gel alone group but abundant in the bFGF-Chitosan gel group (Fig. 3D and S5D). The density of BrdU⁺/Tuj1⁺ cells in the stroke cavity was significantly higher in the bFGF-Chitosan gel group compared with that in the stroke alone or the chitosan gel alone group (Fig. 3E). These results indicated that bFGF-Chitosan gel facilitated the production of new-born immature neurons in the stroke cavity.

Previous studies have demonstrated the extremely limited generation and survival of adult-born neurons after stroke [41]. To investigate the long-term effect of bFGF-Chitosan gel on the survival of new-born neurons after stroke, we prepared the coronal brain sections and performed immunofluorescence staining to detect BrdU and NeuN (a marker for mature neurons) on day 63 post-stroke. BrdU⁺/NeuN⁺ new-born neurons were detected only in the stroke cavity of the bFGF-Chitosan gel mice (Fig. 3F and G), whereas none was observed in the stroke alone group or the chitosan gel alone group (Fig. S5E). Collectively, these results indicated that the appropriately implantation of bFGF-Chitosan gel into the stroke cavity can activate neuroblasts in the SVZ, induce neuroblasts migration toward the stroke cavity, and enhance the maturation and long-term survival of neurons in the stroke cavity (Fig. 3H).

3.4. Synaptogenesis induced by bFGF-Chitosan gel in stroke cavity contributes to restoration of sensorimotor function after ischemic stroke

Synapses are essential for neurotransmission. We next tested whether bFGF-Chitosan gel also promotes synaptogenesis in the stroke cavity. The synaptic vesicle glycoprotein 2A (SV2A) is a highly conserved 12 transmembrane glycoproteins ubiquitously expressed in essentially all presynaptic vesicles [42–44]. SV2A can be visualized and quantified by PET/CT imaging with the novel SV2A specific radio ligand [¹⁸F] SDM-8, which have been widely used as a suitable biomarker for synaptic density in vivo [45]. On day 63 post-stroke, the [¹⁸F] SDM-8 tracer was administrated via tail vein injection, and PET/CT was performed after 60 min. In the stroke alone group, the [¹⁸F] SDM-8 uptake in the stroke cavity was markedly decreased (Fig. 4A), indicating a significant SV2A loss after stroke. Rats treated with bFGF-Chitosan gel showed increased [¹⁸F] SDM-8 binding in the stroke cavity, and the SUVR value was significantly higher compared with that in the stroke alone group or the chitosan gel alone group (Fig. 4B). After PET/CT imaging, rat brain was collected and immunostained for SV2A to further verify SV2A expression in the stroke cavity at the morphological level (Fig. S6). SV2A was highly expressed in the motor cortex of sham rat (34.75 ± 1.75), whereas almost no SV2A positive synapses was detected in the stroke cavity in the stroke alone group (1.33 ± 0.59) or the chitosan gel alone group (2.75 ± 0.75). In the bFGF-Chitosan gel group (11.75 ± 1.55), SV2A mean fluorescence intensity was significantly



(caption on next page)

Fig. 4. Synaptogenesis induced by bFGF-Chitosan gel in stroke cavity contributes to restoration of sensorimotor function after ischemic stroke. (A) Representative image of SV2A PET/CT in each group on day 63 post-stroke. (B) Quantification of SUVR in each group on day 63 post-stroke. $*P < 0.05$, $***P < 0.001$, one-way ANOVA and post-hoc Bonferroni tests, $n = 4$. (C) Anterograde synapses identified by the co-localization of new-born neurons with SV2A/synapsinI, and retrograde synapses identified by co-localization of new-born neurons with PSD95 in stroke cavity on day 63 post-stroke. (D) Schematic diagram of the anterograde and retrograde synaptic connection. (E) Representative ultra-structures images of synapses in the stroke cavity on day 63 post-stroke. At, axonal terminal; Den, dendrite; Red arrows, synaptic cleft; Red circle, gold particles. (F) Quantification of synapses in the stroke cavity in per field on day 63 post-stroke. $*P < 0.05$, $**P < 0.01$, one-way ANOVA and post-hoc Dunnett's T3 test. $n = 4$ in each group. (G) Disruption of synaptic function in the stroke cavity prevents some degree of sensorimotor recovery after stroke. $**P < 0.01$, $***P < 0.001$, bFGF-chitosan + TeLC-mCherry group compared with the sham + TeLC-mCherry group. $#P < 0.05$, $###P < 0.001$, bFGF-chitosan + TeLC-mCherry group compared with the bFGF-chitosan + mCherry, two-way ANOVA. $n = 5$ in each group. Data are presented as mean \pm SEM.

increased (bFGF-Chitosan gel group vs. stroke alone group, $P < 0.001$; bFGF-Chitosan gel group vs. chitosan gel alone group, $P < 0.01$), although it was still lower than that in the sham group (bFGF-Chitosan gel group vs. sham group, $P < 0.001$). Overall, the radiographic and immunofluorescent data suggested that bFGF-Chitosan gel promoted synaptic formation in the stroke cavity after ischemic injury.

To determine the synaptic connection among newly born neurons in the stroke cavity, the expression of the synaptic marker and spatial localization with new-born neurons were examined in the stroke cavity on day 63 post-stroke. Anterograde synaptic connections to BrdU⁺/Tuj1⁺ new-born neurons in the stroke cavity were identified by co-localization with the presynaptic marker SV2A and SynapsinI respectively. Moreover, retrograde synaptic formation onto these BrdU⁺/Tuj1⁺ new-born neurons was identified by co-localization with the postsynaptic marker PSD95. The three-dimensional reconstruction images revealed synaptic formation inside or on the surface of new-born neurons (Fig. 4C and D). These results indicated that bFGF-Chitosan gel induced new-born neurons to establish anterograde and retrograde synaptic connections, and participate in synaptic input and synaptic output respectively.

To further investigate the synaptic ultrastructure between new-born neurons in the stroke cavity, MAP2 immunohistochemistry combined with transmission electron microscope were employed. In the sham group, numerous typical axon-dendrite synapses were observed in motor cortex. In the stroke alone group and the chitosan gel alone group, the stroke cavity had no synaptic elements, but only residual mitochondria, ruptured axial membrane, and collagen fibers. In the bFGF-Chitosan gel group, regenerated tissue exhibited a loose structure and typical axon-dendrite synapses with clear synaptic vesicles in axonal terminal and MAP2⁺gold particles in dendrite. A single dendrite surrounded by multiple presynaptic components was readily detected, which agreed with the characteristic of immature pyramidal neurons (Fig. 4E). Compared with the stroke alone group or the chitosan gel alone group, the synapse number in the stroke cavity was significantly higher in the bFGF-Chitosan gel group (Fig. 4F). The immuno-electron microscopy results directly supported synaptic rearrangement during regenerative process.

To address directly whether synaptogenesis induced by bFGF-Chitosan gel is relevant to functional recovery after stroke, tetanus toxin light chain (TeLC) was next employed to silence synaptic function by inhibiting synaptic vesicular exocytosis [46,47]. To specifically target synapses in the stroke cavity, rAAV-hSyn-TeLC-P2A-mCherry was injected into the stroke cavity on day 42 post-stroke. rAAV-hSyn-mCherry, expressing only mCherry, was used as a control virus (Fig. S7A). In the sham group, post histology confirmed the expression of AAV-mCherry in NeuN positive neurons in the motor cortex (Fig. S7B), and TeLC expression caused an impairment in contralateral forelimb sensorimotor function three weeks after virus injection, confirming the sufficient synaptic disruption mediated by TeLC (Fig. 4G). In mice injected with the control rAAV-hSyn-mCherry, the sensorimotor function improvement induced by bFGF-Chitosan gel unaffected, and mice exhibited gradual and persistent functional restoration. However, three weeks after rAAV-hSyn-TeLC-P2A-mCherry injection into the stroke cavity, bFGF-Chitosan gel treated mice showed a significantly higher percentage of foot faults and decreased usage rate and grip strength in

the impaired limb (Fig. 4G), indicating that TeLC expression partly blocks sensorimotor function recovery induced by bFGF-Chitosan gel. These behavioral results demonstrated that disruption of synaptic function specifically in the stroke cavity prevented some degree of sensorimotor recovery after stroke. Overall, bFGF-Chitosan gel induced synaptic formation in the stroke cavity, rebuilt synaptic connection among new-born neurons, and participated in sensorimotor recovery after ischemic stroke.

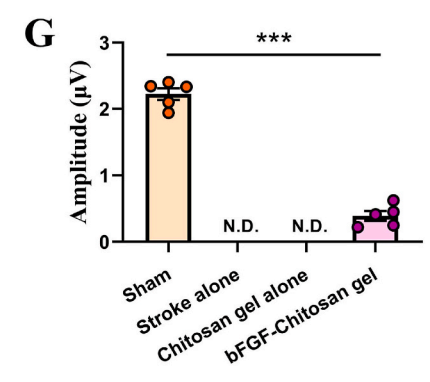
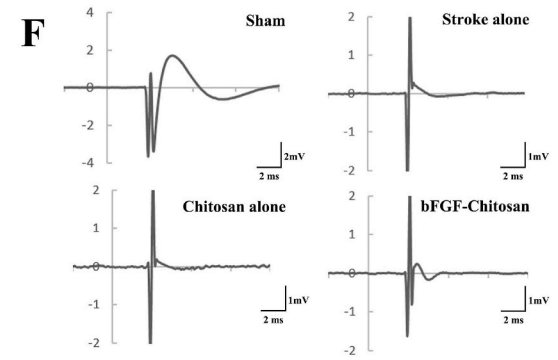
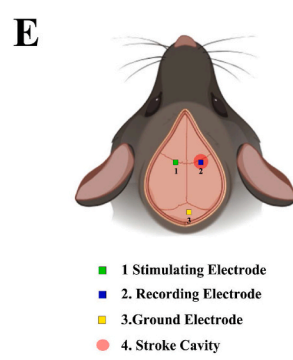
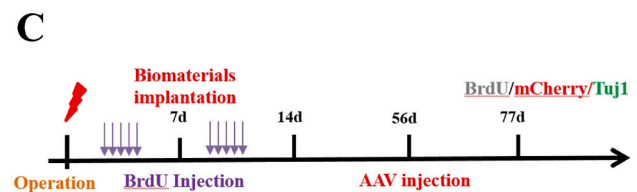
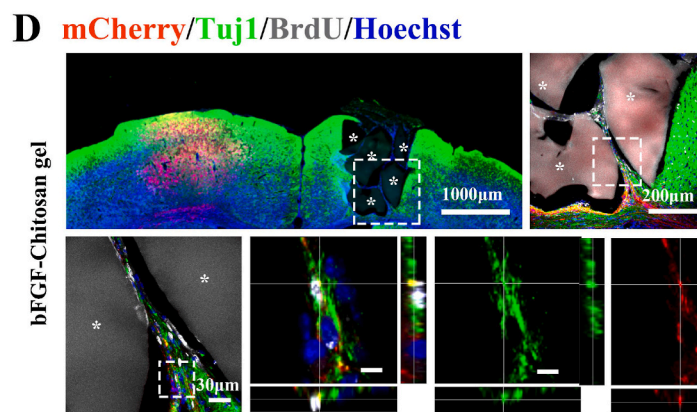
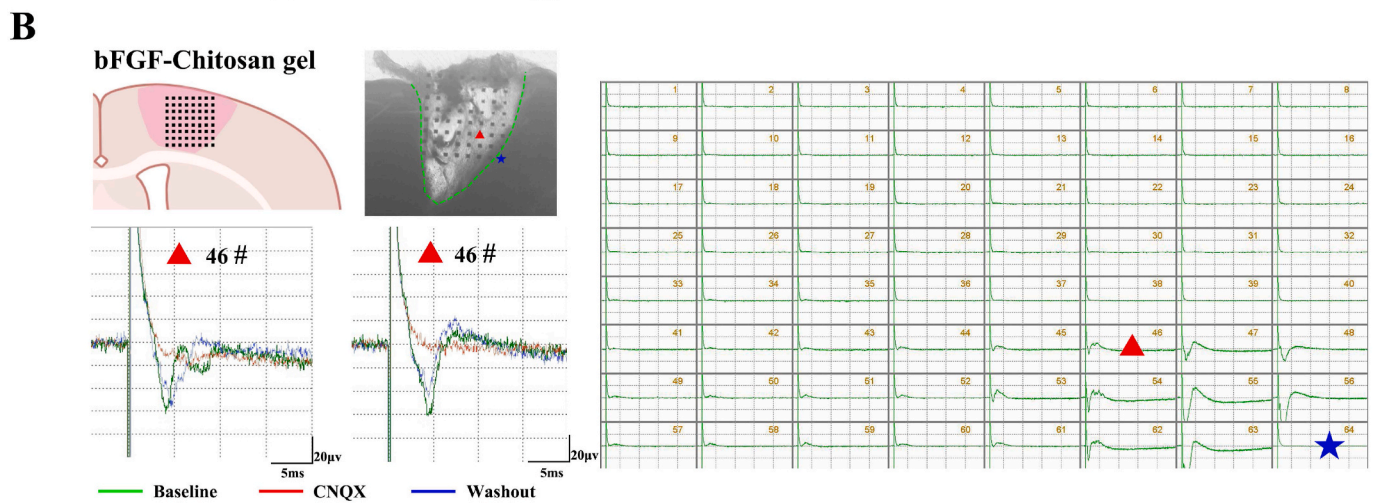
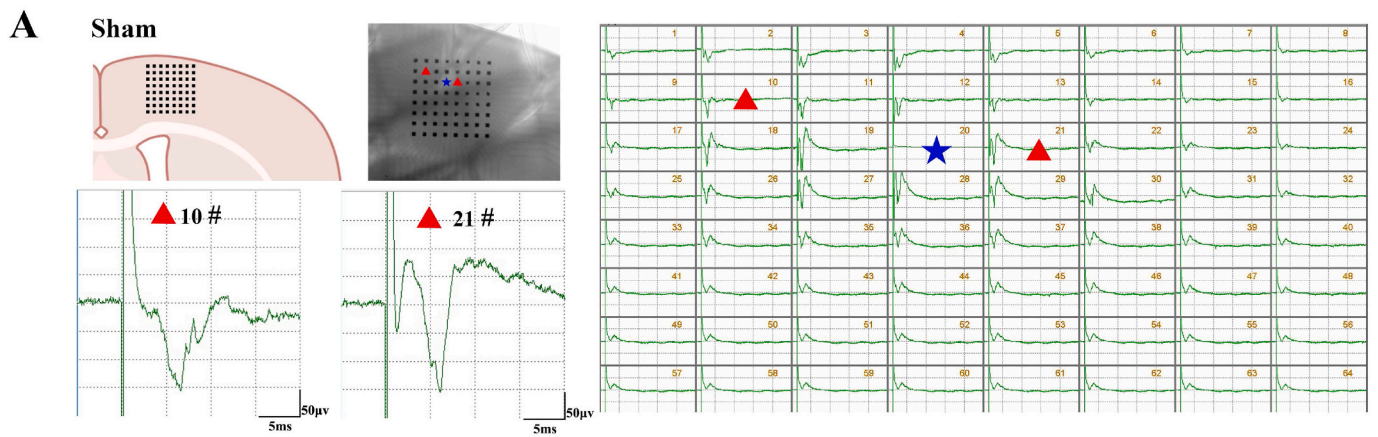
3.5. bFGF-Chitosan gel reconstructs functional neural circuits after ischemic stroke

To determine whether new-born neurons in the stroke cavity of bFGF-Chitosan gel group can integrate into the host brain in the adjacent region, MED64 system was used to record the electrophysiological connectivity of the new neural networks. In the sham group, stimulation of the host motor cortex elicited multisite neural responses in adjacent cortex (Fig. 5A). On day 63 post-stroke, a microelectrode was placed on a brain slice including the regenerated tissue in the stroke cavity and the adjacent host cortex of bFGF-Chitosan gel group, and typical fEPSPs were recorded in the regenerated tissue when the adjacent host motor cortex was stimulated. Moreover, the fEPSPs could be blocked by TTX, and AMPA receptor antagonist CNQX respectively (Fig. 5B). These results indicated that bFGF-Chitosan gel promoted AMPA receptor-mediated synaptic connections between new-born neurons in the stroke cavity and the adjacent host brain.

To further investigate the ability of new-born neurons in the stroke cavity to receive long-distance projections from the contralateral cortex, anterograde tracing virus AAV2/9-hSyn-mCherry was injected into II-III layer of contralateral motor cortex on day 56 post-stroke in the bFGF-Chitosan gel group (Fig. 5C). Three weeks after injection, numerous mCherry positive fibers from left motor cortex extended to the stroke cavity through the corpus callosum, and mCherry positive fibers formed close contact (likely synaptic) with BrdU⁺/Tuj1⁺ new-born neurons in the stroke cavity (Fig. 5D). In addition, our electrophysiology in vivo results showed that typical field postsynaptic potentials (fPSPs) were recorded in the stroke cavity in the bFGF-Chitosan gel group when electrical stimulation was applied on the contralateral motor cortex, while the fPSPs amplitude was significantly decreased compared with that in the sham group (2.22 ± 0.09 vs. 0.39 ± 0.07 mV, $P < 0.001$). By contrast, no fPSPs was recorded in the stroke alone group or the chitosan gel alone group (Fig. 5E–G). The morphological and electrophysiological results indicated that bFGF-Chitosan gel promoted regenerated neurons in the stroke cavity to receive long-distance fiber projections from the contralateral motor cortex. Overall, these data suggested that new-born neurons in the stroke cavity can reconstruct functional neural circuits with host brain after ischemic stroke.

3.6. New-born neurons in stroke cavity partly derived from Nestin lineage cells in SVZ and contribute to functional recovery

To analyze the origin of new-born neurons in the stroke cavity, Nestin^{CreERT2}-tdTomato transgenic mice were used for neural lineage tracing (Fig. 6A). Tamoxifen induce indelible tdTomato expression in Nestin-NSCs and their progeny (Fig. 6B). After seven days of clearing of



(caption on next page)

Fig. 5. bFGF-Chitosan gel reconstructs functional neural circuits after ischemic stroke.

(A) Electro-physiological recordings demonstrate the formation of intra-nascent neural networks on day 63 post-stroke. MED64 array was placed on the motor cortex in sham group. When stimulated the motor cortex (blue star), multiple places were activated in the adjacent area (red triangle). (B) MED64 array was partly on the host's uninjured cortex and partly on the stroke cavity in the bFGF-Chitosan gel group. When stimulated the host's uninjured area (blue star), multiple places were activated in the regenerated area (red triangle), indicative of functional connection between nascent neural network with host. Red triangle, a fEPSP recorded at electrode 46, could be suppressed by TTX (0.5 mM), and CNQX (10 mM). (C) Timeline of experimental procedure for anterograde tracing to detect cortical connections between new-born neurons in the stroke cavity and the contralateral motor cortex. (D) mCherry positive fibers form close contact (likely synaptic) with BrdU⁺/Tuj1⁺ new-born neurons in the stroke cavity in the bFGF-Chitosan gel group on day 77 post-stroke. (E) Schematic diagram of the electrophysiological test in vivo on day 63 post-stroke. (F) When stimulated the host's contralateral motor cortex, typical fPSPs were recorded in the ipsilateral motor cortex in the sham group and the stroke cavity in the bFGF-Chitosan gel group, while no fPSPs was recorded in the stroke alone group or the chitosan gel alone group. fPSPs, field postsynaptic potentials. (G) Quantification of fPSPs amplitude in each group on day 63 post-stroke. *** $P < 0.001$, independent-samples T test, $n = 5$ in each group. Schematic diagram was created with BioRender.com.

Tamoxifen, photothrombotic cortical infarcts were induced, gel was implanted in the stroke cavity on day 7 post-stroke, and then brain tissue was collected on day 14, 35, and 63 post-stroke. Stroke induced a robust migration of tdTomato⁺ cells to the peri-infarct cortex on day 14 post-stroke, and no such migration was observed in the contralateral hemisphere (Fig. 6C). Brain tissue was stained to examine expression of an array of differentiation stage-specific makers in lineage-traced cells (Fig. 6D). On day 14 post-stroke, the majority of tdTomato⁺ cells in the peri-infarct cortex expressed NPCs-associated markers CD133, Sox2 and MASH1 respectively. Compared with that in the stroke alone group, mice treated with bFGF-Chitosan gel exhibited an increase in the cell density of NPCs among tdTomato⁺ cells in the peri-infarct cortex (stroke alone group vs. bFGF-Chitosan gel group: tdTomato⁺/CD133⁺ 852.00 ± 42.52 vs. 1032.00 ± 40.00/mm², $P < 0.05$; tdTomato⁺/Sox2⁺ 704.00 ± 40.82 vs. 904.00 ± 33.47/mm², $P < 0.01$; tdTomato⁺/MASH1⁺ 560.00 ± 42.33 vs. 720.00 ± 29.93/mm², $P < 0.05$, Fig. 6E). In addition, differential rate of NPCs among tdTomato⁺ cells increased in the bFGF-Chitosan group, although no significant difference between two groups (Fig. 6F). These results indicated that bFGF-Chitosan gel induced migration of NPCs derived from Nestin lineage from the SVZ to the peri-infarct cortex.

To determine whether tdTomato⁺ cells could mature into neurons in the stroke cavity, the expression of neuronal markers in the tdTomato-labeled cells was examined. After four weeks of bFGF-Chitosan gel implantation, tdTomato⁺ cells were primarily distributed at the bottom of the stroke cavity, where tdTomato⁺ cells co-expressed the mature neuronal marker NeuN (Fig. 7A). After eight weeks of bFGF-Chitosan gel implantation, tdTomato⁺ cells were widely distributed in the whole stroke cavity, and the density of tdTomato⁺/NeuN⁺ mature neurons was significantly higher than that of four weeks after gel implantation (8 weeks 61.54 ± 6.28 vs. 4 weeks 26.92 ± 7.36 mm², $P < 0.05$, Fig. 7B). Furthermore, these tdTomato⁺/NeuN⁺ neurons co-expressed the superficial cortical layer (II-IV) neuronal marker special AT-rich sequence-binding protein 2 (SATB2) and the deep cortical layer (V-VI) neuronal marker COUP-TF interacting protein 2 inhibitory neuronal (CTIP2) respectively (Fig. 7C). These tdTomato⁺/NeuN⁺ neurons also co-expressed the inhibitory neuronal marker gamma-aminobutyric acid (GABA) and excitatory neuronal marker Ca/calmodulin-dependent kinase II α (CAMKII α) (Fig. 7D). Collectively, these results indicated that bFGF-Chitosan gel induced Nestin lineage cells in the SVZ to migrate toward stroke cavity, and differentiate into mature neurons with original diverse phenotype in the motor cortex.

Finally, to investigate whether the new-born neurons derived from Nestin lineage cells contributed to the bFGF-Chitosan gel induced sensorimotor improvement, Nestin^{CreERT2}-DTA mice was used to eliminate Nestin lineage cells selectively depending on Cre recombinase expression [35] (Fig. 7E). Tamoxifen induces diphtheria toxin expression under the Nestin promoter, which promotes niacinamide generation and inactivates EF-2, finally blocks cellular protein synthesis, and leads to the death of Nestin lineage cells [35]. Nestin^{CreERT2}-DTA mice injected with corn coil were used as the control. The behavior tests showed that sensorimotor function gradually improved with bFGF-Chitosan gel implantation over time in the wild type mice and

Nestin^{CreERT2}-DTA mice injected with corn coil. After Nestin^{CreERT2}-DTA mice were injected with tamoxifen, Nestin lineage cells were eliminated and no new-born neuron was observed in the stroke cavity until day 63 post-stroke (Fig. 7F and Fig. S8). Mice exhibited behavioral deterioration starting from day 35 post-stroke, and these behavior impairments persisted for up to day 63 post-stroke (Fig. 7G). These results indicated that new-born neurons derived from Nestin lineage cells contributed to the improvement in sensorimotor function induced by bFGF-Chitosan gel after ischemic stroke.

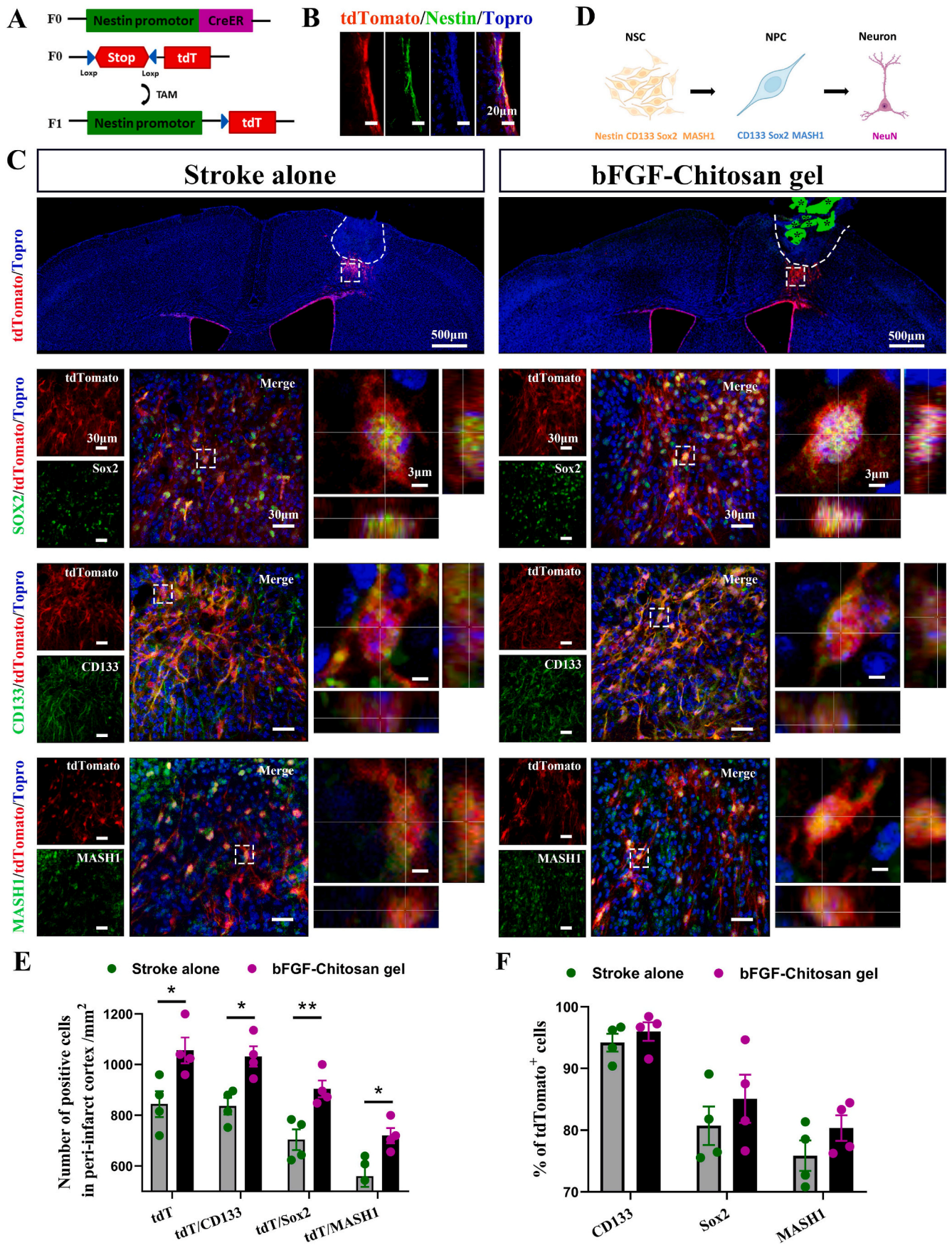
3.7. bFGF-Chitosan gel inhibits microglia activation in peri-infarct cortex after ischemic stroke

To further detect the effects of bFGF-Chitosan gel on immune cells, we perform IBA1 staining on day 63 post-stroke (Fig. 8). In the sham group, IBA1⁺ microglia displayed a resting state with small bodies and well ramified processes. In the stroke alone group, significant increase in the number of IBA1⁺ microglia was observed in the peri-infarct region. Analysis of 3D-reconstructions of the microglia showed swollen cell bodies and short, thicken processes. Sholl analysis confirmed a global decrease in the number of branch intersections and length of branches, which indicative of decreased branching complexity and highly hypertrophic activation state of microglia on day 63 after stroke. By contrast, transplantation of bFGF-Chitosan gel and chitosan alone gel significantly reduced the density of IBA1⁺ microglia and simultaneously accompanied with restoration in the branching complexity. These data suggested that bFGF-Chitosan gel suppressed activation of microglia in the peri-infarct cortex after ischemic stroke.

4. Discussion

The present study reports the mechanism of implantation of bFGF-Chitosan gel in the stroke cavity improves sensorimotor functional recovery in adult rodents. Our study demonstrates that bFGF-Chitosan gel suppress activation of microglia, and promotes angiogenesis, endogenous neurogenesis and synaptogenesis after ischemic stroke. Essentially, bFGF-Chitosan gel induces the formation of new-born vascular networks, activates endogenous NPCs, guides the directional migration toward the stroke cavity, and differentiation into mature neurons, the formation of functional synaptic connection, and the reconstruction nascent neural networks. Additionally, synaptogenesis induced by bFGF-Chitosan gel in the stroke cavity and Nestin lineage cells contribute to the improvement of sensorimotor function respectively after ischemic stroke.

Angiogenesis is a key feature of ischemic stroke recovery, including the process of formation, differentiation, and maturation of neo-vascularization [48]. Ischemic penumbra is an active zone of angiogenesis, involved in vascular endothelial cell proliferation and increased vascular density [49,50]. Experimental animal and clinical data have demonstrated that angiogenesis induction and new vessel generation contribute to neurorepair processes and functional recovery [51,52]. Nih et al. [34] demonstrated that a VEGF-containing hydrogel induced the formation of mature and highly developed vascular bed within the



(caption on next page)

Fig. 6. bFGF-Chitosan gel induces migration of neural precursors derived from Nestin lineage toward peri-infract cortex.

(A) Schematic diagram of Nestin^{CreERT2}-tdTomato transgenic mice. (B) Representative immunofluorescence images showed tdTomato⁺ cells express Nestin in SVZ (tdTomato/Nestin/topro). (C) Representative immunofluorescence images from peri-infract cortex of tdTomato⁺ cells with various neuronal progenitor markers CD133, SOX2, and MASH1 on day 14 post-stroke. (D) Schematic of differentiation stages as defined by marker expression. Neural stem cells (NSC) produce neuronal progenitor cells (NPCs), which give rise to neurons. (E) Quantitative analyses of cell density of tdTomato⁺, tdTomato⁺/CD133⁺, tdTomato⁺/SOX2⁺, and tdTomato⁺/MASH1⁺ in peri-infract cortex on day 14 post-stroke. **P* < 0.05, ***P* < 0.01, independent-samples T test, *n* = 4 in each group. (F) Quantitative analyses of differential rate of NPCs among tdTomato⁺ cells on day 14 post-stroke. Independent-samples T test, *n* = 4 in each group. Schematic diagram was created with BioRender.com.

stroke cavity. In the present study, we provide compelling evidence demonstrating that bFGF-Chitosan gel enhances angiogenesis through three methods. First, BrdU/GluT1 immunofluorescence staining revealed a profound increase of neovascular formation in the stroke cavity. Second, lection injection and morphological results showed the functional vascular network had integrated into the host vascular system. Third, LSCI *in vivo* confirmed a significant improvement of restoration of cerebral blood flow in and around the stroke cavity. LSCI has been used to visualize the changes of cerebral blood flow throughout the ischemic territory in stroke models of the rodents [53]. After ischemic stroke, the spatial blood flow gradient could be visualized because LSCI can provide a dynamic view of stroke cavity and peri-infract cortex [54]. In our study, the blood flow was increased in the chitosan gel alone group, this may be because that chitosan alone can be used as temporary framework to mimic the natural extracellular matrix and microenvironment for supporting newly generated vessels, which facilitate endothelial cell adhesion, proliferation, and differentiation. Meanwhile, controlled release bFGF by chitosan further promote angiogenesis, demonstrated by more new-born vessels and markedly increased blood flow restoration. Because angiogenesis is coupled with neurogenesis [38], we believe that angiogenesis induced by bFGF-Chitosan gel provides trophic support for regenerating tissue in the stroke cavity to promote long-term survival of new-born neurons.

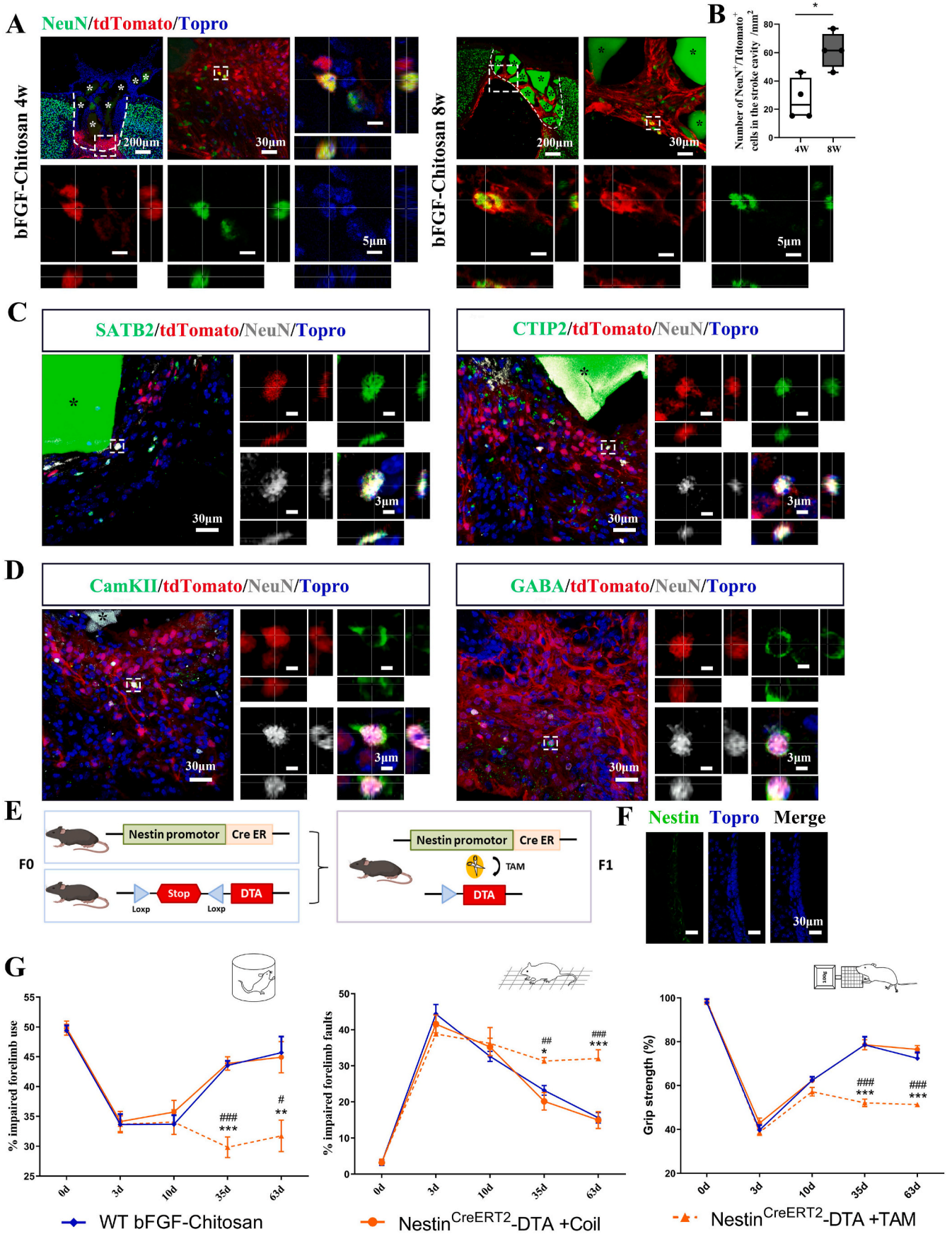
The cortex is a non-neurogenic region, and its neurogenic potential becomes minimal in adulthood [55,56]. Normally, the predominant progeny arising from the SVZ migrate toward the olfactory bulb, whereas cortical injury induce SVZ-derived NPCs to migrate toward the injury site [57]. Accordingly, we observed the NPCs exhibited a bipolar morphology and migrated toward the peri-infract cortical region, and bFGF-Chitosan gel enhanced the ectopic migration. Utilizing indelible lineage tracing technique and extensive phenotyping, we further identified that NPCs partly originate from Nestin lineage cells in the SVZ region. In addition, previous studies have proposed that endogenous NPCs are rather derived from regionally-activated cell *in situ* [58]. The other potential neurogenic cells in the cortex included oligodendrocyte progenitors [59], peripheral cells [60–62], and reactive astrocytes [63–65]. Further research is necessary to fully clarify whether these potential neurogenic cells serve as additional sources of NPCs and migration mechanism driven by the bFGF-Chitosan gel.

Indeed, new-born neurons face challenges of long time surviving in harsh environment after a stroke. In our present study, BrdU⁺/NeuN⁺ and tdTomato⁺/NeuN⁺ new-born neurons were observed in the stroke cavity until 2 months after bFGF-Chitosan gel implantation. Mammalian brains commonly show I–VI layer neocortex, and each layer has a specific morphology, function and synaptic connection [66,67]. Our immunofluorescence staining showed that the new-born neurons expressed the superficial (tdTomato⁺/SATB2⁺) and deep (tdTomato⁺/CTIP2⁺) cortical layer neuronal markers, which is important for the reconstruction of appropriate neural circuit and the attainment of complex function after a stroke. However, even if there were layers II–VI new-born neurons in stroke cavity, their distribution was distorted by the chitosan gel and could hardly achieve the laminar formation and layer architecture like that in sham cortex. In our previous study, bFGF-Chitosan gel induced SVZ-derived NSCs to differentiate into mature neurons with diverse phenotypes *in vitro* [20]. Consistent with these *in vitro* findings, bFGF-chitosan-gel-induced new-born neurons in the stroke cavity comprised inhibitory GABA neurons and excitatory CamKII α glutamatergic neurons. In the mammalian brain, glutamatergic

neurons account for approximately 80 % and establish functional connections with other brain regions [68]. Notably, our pharmacological assay demonstrated that fEPSPs recorded in the stroke cavity could be suppressed by AMPA/kainate receptor antagonist CNQX, indicating the involvement of excitatory glutamatergic neurons within nascent neural networks. In subsequent study, the electrophysiological characteristics of new-born neurons will be further clarified by patch clamp technology at the individual cell level.

Ischemic stroke leads to synaptic dysfunction and degradation, ultimately resulting in the loss of synapses [69]. Synapses serve as the major site of information transmission and functional connection between neurons. Thus, synaptogenesis is critical for brain repair following cerebral ischemic stroke. Synaptogenesis involves synaptic formation, synaptic connection, and synaptic integration [70]. Our findings provide robust evidence that bFGF-Chitosan gel enhances three key processes of synaptogenesis. Expression of synaptic marker SV2A within the stroke cavity, detected by [¹⁸F] SDM-8 PET/CT and morphology analysis, indicated the formation of synaptic components. Next, the localization analysis revealed anterograde and retrograde synaptic connection with new-born neurons, reflected as the expression of presynaptic marker, SV2A, Synapsin I, as well as the postsynaptic marker PSD95 within or on the surface of new-born neurons. Moreover, the immunoelectronic microscope results further revealed the ultrastructure of synapses in the stroke cavity. Finally, functional synaptic integration into the host neural circuitry was confirmed. The reconstruction of local circuitry was supported by MED64 assay, indicating functional integration from neighboring neurons in the adjacent cortex to the new-born neurons in the stroke cavity. In addition to local connections, long-distance cortical–cortical connections were identified through AAV anterograde tracing and electrophysiology *in vivo*, providing the morphological and functional reconstruction of fiber projections from the contralateral motor cortex.

Preliminary evidence suggested an association between post-stroke neurogenesis and functional recovery. After cryogenic cortical injury in neonatal mice, NCad-mRADA promoted the migration of NPCs toward injury cortex and differentiation into mature neurons [26]. The ablation of endogenous NSCs in Nestin^{CreERT2}-DTA mice blocked the NCad-mRADA treatment-induced improvement in sensorimotor function [35]. After cortical ischemic stroke, motor recovery was significantly impaired in GFAP-TK mice treated with ganciclovir treatment to eliminate endogenous NSCs [71]. Similarly, our findings demonstrated that by eliminating Nestin lineage cells in Nestin^{CreERT2}-DTA mice, bFGF-Chitosan gel-induced sensorimotor function recovery was partly blocked, providing direct evidence that endogenous Nestin lineage cells contribute to the functional recovery induced by bFGF-Chitosan gel. However, ablation of endogenous NSCs prior to cortical injury, using genetic and pharmacological approaches, may potentially have adverse effects on neuroprotection while inhibiting neurogenesis [72]. To overcome these limitations, some researchers have proposed silencing neuronal or synaptic function, rather than eliminating endogenous NSCs. Liang et al. [41] employed tetanus toxin (TeNT) to inhibit vesicular transmitter release, then silence synaptic function of SVZ-derived neurons. They discovered that TeNT significantly inhibited the disruption of synaptic formation, specifically in SVZ-derived neurons, thereby preventing a certain degree of recovery after stroke. Additionally, TeLC is also an effective agent to silence synaptic function by inhibiting synaptic vesicular exocytosis [73,74]. In the present study, TeLC was injected into the stroke cavity to specifically silence synaptic function in



(caption on next page)

Fig. 7. New-born neurons in stroke cavity partly derived from Nestin lineage in SVZ and contribute to functional restoration.

(A) Representative immunofluorescence images from the stroke cavity showing expression of the NeuN in tdTomato⁺ cells at 4w and 8w of bFGF-Chitosan gel implantation (tdTomato/NeuN/topro). (B) Quantitative analyses of cell density of tdTomato⁺/NeuN⁺. $P < 0.05$, independent-samples T test, $n = 4$ in each group. (C) Representative immunofluorescence images from stroke cavity showing expression of SATB2 and CTIP2 in tdTomato⁺ cells at 8w of bFGF-Chitosan implantation. (D) Representative immunofluorescence images from stroke cavity showing expression of CAMKII α and GABA in tdTomato⁺ cells at 8w of bFGF-Chitosan implantation. (E) Schematic diagram of Nestin^{CreERT2}-DTA transgenic mice. (F) After injection with tamoxifen in Nestin-DTA mice, Nestin lineage cells were eliminated. (G) Ablation of Nestin lineage cells prevents some degree of sensorimotor recovery after stroke. * $P < 0.05$, ** $P < 0.01$, *** $P < 0.001$, the Nestin^{CreERT2}-DTA + TAM group compared with the WT bFGF-Chitosan gel group. # $P < 0.05$, ## $P < 0.01$, ### $P < 0.001$, the Nestin^{CreERT2}-DTA + TAM group compared with the Nestin^{CreERT2}-DTA + Coil mice, two-way ANOVA. $n = 5$ in each group. Data are presented as mean \pm SEM. Schematic diagram was created with [BioRender.com](https://www.biorender.com).

A IBA1/Hoechst

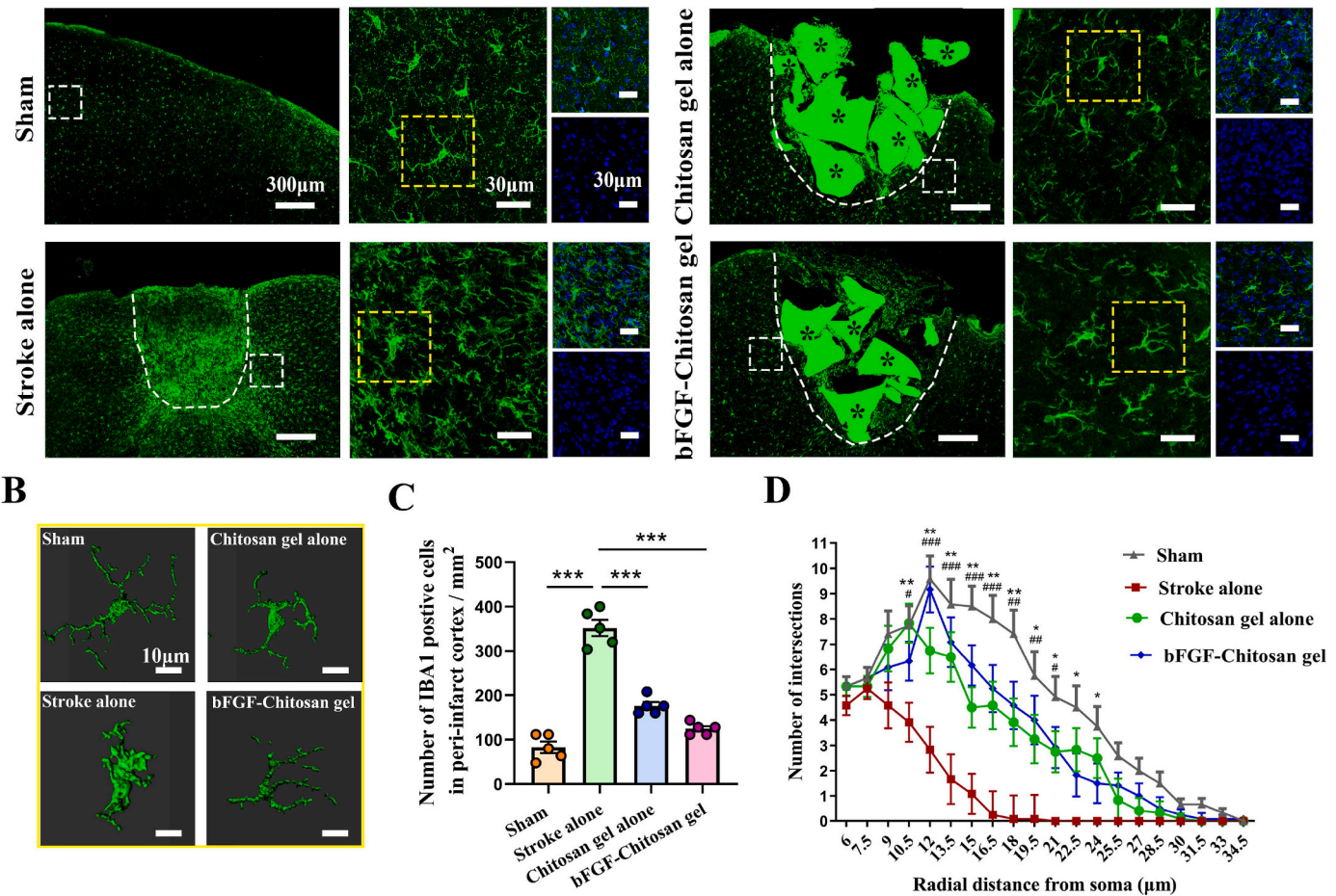


Fig. 8. bFGF-Chitosan gel suppress the activation of microglia in peri-infarct area.

(A) Representative immunofluorescence images of microglia in the peri-infarct cortex on day 63 post-stroke (IBA1/Hoechst). (B) Representative 3D-reconstructions of microglia in each group. (C) Quantitative analyses of cell density of IBA1⁺ in the peri-infarct cortex on day 63 post-stroke. *** $P < 0.001$, one-way ANOVA and post-hoc Bonferroni tests. $n = 5$ in each group. Data are presented as mean \pm SEM. (D) Sholl analysis of microglia in the peri-infarct cortex on day 63 post-stroke. * $P < 0.05$, ** $P < 0.01$, the chitosan gel alone group compared with the stroke alone group. # $P < 0.05$, ## $P < 0.01$, ### $P < 0.001$, the bFGF-Chitosan gel group compared with the stroke alone group, two-way ANOVA, $n = 12$ in each group. Data are presented as mean \pm SEM.

stroke cavity, partially blocking the bFGF-Chitosan gel induced sensorimotor function recovery. Therefore, this work provides a causative link between behavior improvements induced by bFGF-Chitosan gel with synaptic activity in the stroke cavity.

Microglia are the prototypical resident immune cells and the first line of defense against injury in the central nervous system. After ischemic brain injury, microglia cells degenerate in the stroke cavity, while proliferate at the periphery of infarction [75]. Although microglia are reported act as double-edged sword after stroke, chronically activated microglia might play harmful roles in neurogenesis, because these microglia release cytotoxic substances, eliciting inflammation and contributing to death of new-born neurons [76]. Administration of the anti-inflammatory drug or microglial depletion during chronic phase to

reduce microglia activation, increase the number of new neuroblasts and reduce neurological deficits [77–79]. In our present study, the transplanted bFGF-Chitosan gel significantly reduce the density and activation of microglia, and these benefit could also be found in chitosan alone gel group. Our results indicated that chitosan may play an important role in suppress the cytotoxic action of microglia. Indeed, the anti-inflammatory activities of chitosan have been reported in multiple models, included traumatic brain injury [21], Alzheimer’s disease [80], and ischemia and reperfusion injury [81]. Thus, our bioactive materials supply better microenvironment for newborn neurons, which is favor of long-term survive of newborn neurons.

5. Conclusions

The present study report that bFGF-Chitosan gel acts as “brain glue” filling the stroke cavity and improves sensorimotor function recovery after cortical ischemic stroke in rodents. These benefit mechanisms may be possible with new strategies targeting three areas: bFGF-Chitosan gel promotes angiogenesis, revascularization, and restoration of cerebral blood flow in stroke cavity. bFGF-Chitosan gel activates endogenous neurogenesis and guides SVZ-derived NPCs to migrate toward the stroke cavity and differentiate into mature neurons with diverse phenotypes. bFGF-Chitosan gel enhances synaptogenesis and reconstructs nascent neural networks. Our study opens up innovative ideas and methods for the clinical treatment of ischemic stroke.

6. Limitation

Currently, the clinical applications of intraparenchymal (IP) transplantation of biomaterials indeed face several hurdles: Firstly, the removal of necrotic tissue from stroke patients is usually not approved based on current treatment guidelines. Secondly, the most significant hurdle to the clinical use of IP transplantation is the highly invasive nature of the required craniectomy, which could lead to possible complications of infection in stroke patients. Lastly, precise injection into the stroke cavity with biomaterials generally need specialized infrastructure and professional neurosurgeons. However, IP transplantation of biomaterials indeed have numerous advantages including eliminating the need for biomaterials to transverse the blood brain barrier; guaranteed delivery of biomaterials to the stroke cavity, and overcome the potential for off-target problems of systemic delivery [82,83]. Importantly, some recent clinical trials in human and preclinical stroke study in non-human primates have demonstrated that IP delivery appears to be relatively safe and feasible administration route, which deserving of further clinical study [84–86].

CRedit authorship contribution statement

Jiao Mu: Writing – original draft, Validation, Resources, Investigation, Data curation, Conceptualization. **Xiang Zou:** Methodology, Conceptualization. **Xinjie Bao:** Supervision, Project administration, Funding acquisition, Formal analysis, Data curation. **Zhaoyang Yang:** Writing – original draft, Visualization, Resources, Methodology, Investigation, Funding acquisition, Data curation. **Peng Hao:** Validation, Supervision, Project administration, Data curation. **Hongmei Duan:** Visualization, Supervision, Resources, Funding acquisition, Conceptualization. **Wen Zhao:** Validation, Software, Methodology, Formal analysis. **Yudan Gao:** Visualization, Resources, Project administration, Funding acquisition, Conceptualization. **Jinting Wu:** Software, Conceptualization. **Kun Miao:** Visualization, Investigation, Data curation. **Kwok-Fai So:** Writing – review & editing, Validation. **Liang Chen:** Writing – review & editing, Supervision, Resources, Funding acquisition. **Ying Mao:** Writing – review & editing, Visualization, Supervision, Funding acquisition. **Xiaoguang Li:** Writing – review & editing, Supervision, Resources, Funding acquisition, Conceptualization.

Data availability

All data generated or analyzed during this study are included in this published paper.

Ethics approval and consent to participate

All animal procedures were approved by the Institutional Animal Care and Use Committee of Capital Medical University (No. AEE-2022-225 and No. AEEI-2019-151). All experiments were carefully conducted in accordance with the guidelines for Animal Experimentation of Capital Medical University.

Declaration of competing interest

The authors affirm that they have no known financial or interpersonal conflicts that could have appeared to have an impact on the research presented in this study.

Acknowledgements

This study was supported by the National Natural Science Foundation of China, Nos. 31730030 (to XL), 82272171 (to ZY), 82271403 (to XL), 81941011 (to XL), 31971279 (to ZY), 31771053 (to HD), 82472244 (to XZ), 82272116 (to LC); the Natural Science Foundation of Beijing, No. 7222004 (to HD); Science and Technology Innovation Plan of Shanghai Science and Technology Commission, No. 23Y31900300 (to YM). the CAMS Initiative for Innovative Medicine, 2021-1-I2M – 019 (to XB), and National High Level Hospital Clinical Research Funding, 2022-PUMCH-C-042 (to XB). We thank Kun He and Zhihui Xu for technical assistance at PET/CT. We thank Sa Zhang for his help in immuno-electron microscopy.

Appendix A. Supplementary data

Supplementary data to this article can be found online at <https://doi.org/10.1016/j.bioactmat.2024.12.017>.

References

- [1] B.C.V. Campbell, D.A. De Silva, M.R. Macleod, et al., Ischaemic stroke, *Nat. Rev. Dis. Prim.* 5 (1) (2019) 70.
- [2] Y. Jiang, Z. Liu, Y. Liao, et al., Ischemic stroke: from pathological mechanisms to neuroprotective strategies, *Front. Neurol.* 13 (2022) 1013083.
- [3] A. Moretti, F. Ferrari, R.F. Villa, Neuroprotection for ischaemic stroke: current status and challenges, *Pharmacol. Ther.* 146 (2015) 23–34.
- [4] Y. Du, Y. Huo, Q. Yang, et al., Ultrasmall iron-gallic acid coordination polymer nanodots with antioxidative neuroprotection for PET/MR imaging-guided ischemia stroke therapy, *Explorations* 3 (1) (2023) 20220041.
- [5] L. Tang, Y. Yin, H. Liu, et al., Blood-brain barrier-penetrating and lesion-targeting nanoplatforms inspired by the pathophysiological features for synergistic ischemic stroke therapy, *Adv. Mater.* 36 (21) (2024) e2312897.
- [6] Z.Z. Hao, J.R. Wei, D. Xiao, et al., Single-cell transcriptomics of adult macaque hippocampus reveals neural precursor cell populations, *Nat. Neurosci.* 25 (6) (2022) 805–817.
- [7] W. Wang, M. Wang, M. Yang, et al., Transcriptome dynamics of hippocampal neurogenesis in macaques across the lifespan and aged humans, *Cell Res.* 32 (8) (2022) 729–743.
- [8] Y. Zhou, Y. Su, S. Li, et al., Molecular landscapes of human hippocampal immature neurons across lifespan, *Nature* 607 (7919) (2022) 527–533.
- [9] O. Lindvall, Z. Kokaia, Neurogenesis following stroke affecting the adult brain, *Cold Spring Harbor Perspect. Biol.* 7 (11) (2015).
- [10] E.M. Purvis, J.C. O'donnell, H.I. Chen, et al., Tissue engineering and biomaterial strategies to elicit endogenous neuronal replacement in the brain, *Front. Neurol.* 11 (2020) 344.
- [11] S. Gnani, C. Barwig, T. Freier, et al., The use of chitosan-based scaffolds to enhance regeneration in the nervous system, *Int. Rev. Neurobiol.* 109 (2013) 1–62.
- [12] D.D. Ojeda-Hernández, A.A. Canales-Aguirre, J. Matias-Guiu, et al., Potential of chitosan and its derivatives for biomedical applications in the central nervous system, *Front. Bioeng. Biotechnol.* 8 (2020) 389.
- [13] Y. Kim, Z. Zharkinbekov, K. Raziyeva, et al., Chitosan-based biomaterials for tissue regeneration, *Pharmaceutics* 15 (3) (2023).
- [14] S.M. Mawazi, M. Kumar, N. Ahmad, et al., Recent applications of chitosan and its derivatives in antibacterial, anticancer, wound healing, and tissue engineering fields, *Polymers* 16 (10) (2024).
- [15] N. Desai, D. Rana, S. Salave, et al., Chitosan: a potential biopolymer in drug delivery and biomedical applications, *Pharmaceutics* 15 (4) (2023).
- [16] M.P. Patel, R.R. Patel, J.K. Patel, Chitosan mediated targeted drug delivery system: a review, *J. Pharm. Pharmaceut. Sci.* 13 (4) (2010) 536–557.
- [17] S. Alizadeh, A. Samadikuchaksaraei, D. Jafari, et al., Enhancing diabetic wound healing through improved angiogenesis: the role of emulsion-based core-shell micro/nanofibrous scaffold with sustained CuO nanoparticle delivery, *Small* (2024) e2309164.
- [18] R.T. Böttcher, C. Niehrs, Fibroblast growth factor signaling during early vertebrate development, *Endocr. Rev.* 26 (1) (2005) 63–77.
- [19] H. Duan, S. Li, P. Hao, et al., Activation of endogenous neurogenesis and angiogenesis by basic fibroblast growth factor-chitosan gel in an adult rat model of ischemic stroke, *Neural Regen Res.* 19 (2) (2024) 409–415.
- [20] T. Bai, H. Duan, B. Zhang, et al., Neuronal differentiation and functional maturation of neurons from neural stem cells induced by bFGF-chitosan controlled release system, *Drug Deliv. Transl. Res.* 13 (9) (2023) 2378–2393.

- [21] P. Hao, H. Duan, F. Hao, et al., Neural repair by NT3-chitosan via enhancement of endogenous neurogenesis after adult focal aspiration brain injury, *Biomaterials* 140 (2017) 88–102.
- [22] J. Mu, L. Hao, Z. Wang, et al., Visualizing Wallerian degeneration in the corticospinal tract after sensorimotor cortex ischemia in mice, *Neural Regen Res.* 19 (3) (2024) 636–641.
- [23] F. Yan, X. Cheng, M. Zhao, et al., Loss of Wip1 aggravates brain injury after ischaemia/reperfusion by overactivating microglia, *Stroke Vasc. Neurol.* 6 (3) (2021) 344–351.
- [24] R. Muñoz-Castañeda, B. Zingg, K.S. Matho, et al., Cellular anatomy of the mouse primary motor cortex, *Nature* 598 (7879) (2021) 159–166.
- [25] J. Mu, M. Li, T. Wang, et al., Myelin damage in diffuse axonal injury, *Front. Neurosci.* 13 (2019) 217.
- [26] M. Beyazova, M. Zinnuroglu, H. Emmez, et al., Intraoperative neurophysiological monitoring during surgery for tethered cord syndrome, *Turk Neurosurg* 20 (4) (2010) 480–484.
- [27] C. Li, X. Zhu, C.M. Lee, et al., A mouse model of complete-crush transection spinal cord injury made by two operations, *Ann. Transl. Med.* 8 (5) (2020) 210.
- [28] Y. Kong, L. Cao, F. Xie, et al., Reduced SV2A and GABA(A) receptor levels in the brains of type 2 diabetic rats revealed by [(18)F]SDM-8 and [(18)F]flumazenil PET, *Biomed. Pharmacother.* 172 (2024) 116252.
- [29] J. Zhang, J. Wang, X. Xu, et al., In vivo synaptic density loss correlates with impaired functional and related structural connectivity in Alzheimer's disease, *J. Cerebr. Blood Flow Metabol.* 43 (6) (2023) 977–988.
- [30] H. Duan, X. Li, C. Wang, et al., Functional hyaluronate collagen scaffolds induce NSCs differentiation into functional neurons in repairing the traumatic brain injury, *Acta Biomater.* 45 (2016) 182–195.
- [31] Z. Yang, A. Zhang, H. Duan, et al., NT3-chitosan elicits robust endogenous neurogenesis to enable functional recovery after spinal cord injury, *Proc. Natl. Acad. Sci. U.S.A.* 112 (43) (2015) 13354–13359.
- [32] N. Belforte, J. Agostinone, L. Alarcon-Martinez, et al., AMPK hyperactivation promotes dendrite retraction, synaptic loss, and neuronal dysfunction in glaucoma, *Mol. Neurodegener.* 16 (1) (2021) 43.
- [33] H.W. Morrison, J.A. Filosa, A quantitative spatiotemporal analysis of microglia morphology during ischemic stroke and reperfusion, *J. Neuroinflammation* 10 (2013) 4.
- [34] L.R. Nih, S. Gojgini, S.T. Carmichael, et al., Dual-function injectable angiogenic biomaterial for the repair of brain tissue following stroke, *Nat. Mater.* 17 (7) (2018) 642–651.
- [35] Y. Ohno, C. Nakajima, I. Ajioka, et al., Amphiphilic peptide-tagged N-cadherin forms radial glial-like fibers that enhance neuronal migration in injured brain and promote sensorimotor recovery, *Biomaterials* 294 (2023) 122003.
- [36] S. Li, P. Hao, F. Hao, et al., Pathological changes in rats with ischemic stroke induced by improved photochemical embolization, *Chin. J. Tissue Eng. Res.* 26 (2) (2022) 218.
- [37] Y. Liang, P. Hao, H. Duan, et al., Pathological and behavioral changes after ischemic stroke in adult mice 24 (35) (2020) 5625.
- [38] L. Ruan, B. Wang, Q. Zhuge, et al., Coupling of neurogenesis and angiogenesis after ischemic stroke, *Brain Res.* 1623 (2015) 166–173.
- [39] J.A. Florian, J.R. Kosky, K. Ainslie, et al., Heparan sulfate proteoglycan is a mechanosensor on endothelial cells, *Circ. Res.* 93 (10) (2003) e136–e142.
- [40] M.Y. Pahakis, J.R. Kosky, R.O. Dull, et al., The role of endothelial glycocalyx components in mechanotransduction of fluid shear stress, *Biochem. Biophys. Res. Commun.* 355 (1) (2007) 228–233.
- [41] H. Liang, H. Zhao, A. Gleichman, et al., Region-specific and activity-dependent regulation of SV2 neurogenesis and recovery after stroke, *Proc. Natl. Acad. Sci. U.S.A.* 116 (27) (2019) 13621–13630.
- [42] A. Bayés, S.G. Grant, Neuroproteomics: understanding the molecular organization and complexity of the brain, *Nat. Rev. Neurosci.* 10 (9) (2009) 635–646.
- [43] K. Buckley, R.B. Kelly, Identification of a transmembrane glycoprotein specific for secretory vesicles of neural and endocrine cells, *J. Cell Biol.* 100 (4) (1985) 1284–1294.
- [44] Z. Cai, S. Li, D. Matuskey, et al., PET imaging of synaptic density: a new tool for investigation of neuropsychiatric diseases, *Neurosci. Lett.* 691 (2019) 44–50.
- [45] S.J. Finnema, N.B. Nabulsi, T. Eid, et al., Imaging synaptic density in the living human brain, *Sci. Transl. Med.* 8 (348) (2016) 348ra396.
- [46] M. Christensen, S.E. Nørr, U. Gether, et al., Direct-Pathway spiny projection neuron inhibition evokes transient circuit imbalance manifested as rotational behavior, *Neuroscience* 453 (2021) 32–42.
- [47] M. Drexel, S. Rahimi, G. Sperk, Silencing of hippocampal somatostatin interneurons induces recurrent spontaneous limbic seizures in mice, *Neuroscience* 487 (2022) 155–165.
- [48] Y. Yang, M.T. Torbey, Angiogenesis and blood-brain barrier permeability in vascular remodeling after stroke, *Curr. Neuropharmacol.* 18 (12) (2020) 1250–1265.
- [49] T. Hayashi, N. Noshita, T. Sugawara, et al., Temporal profile of angiogenesis and expression of related genes in the brain after ischemia, *J. Cerebr. Blood Flow Metabol.* 23 (2) (2003) 166–180.
- [50] H.J. Marti, M. Bernaudin, A. Bellail, et al., Hypoxia-induced vascular endothelial growth factor expression precedes neovascularization after cerebral ischemia, *Am. J. Pathol.* 156 (3) (2000) 965–976.
- [51] J. Krupinski, J. Kaluza, P. Kumar, et al., Role of angiogenesis in patients with cerebral ischemic stroke, *Stroke* 25 (9) (1994) 1794–1798.
- [52] M.R. Williamson, C.J.A. Fuertes, A.K. Dunn, et al., Reactive astrocytes facilitate vascular repair and remodeling after stroke, *Cell Rep.* 35 (4) (2021) 109048.
- [53] S.M. Kazmi, L.M. Richards, C.J. Schrandt, et al., Expanding applications, accuracy, and interpretation of laser speckle contrast imaging of cerebral blood flow, *J. Cerebr. Blood Flow Metabol.* 35 (7) (2015) 1076–1084.
- [54] D.A. Boas, A.K. Dunn, Laser speckle contrast imaging in biomedical optics, *J. Biomed. Opt.* 15 (1) (2010) 011109.
- [55] W. Jiang, W. Gu, T. Brännström, et al., Cortical neurogenesis in adult rats after transient middle cerebral artery occlusion, *Stroke* 32 (5) (2001) 1201–1207.
- [56] S.G. Kernie, J.M. Parent, Forebrain neurogenesis after focal Ischemic and traumatic brain injury, *Neurobiol. Dis.* 37 (2) (2010) 267–274.
- [57] K. Ohira, Injury-induced neurogenesis in the mammalian forebrain, *Cell. Mol. Life Sci.* 68 (10) (2011) 1645–1656.
- [58] S. Fujiwara, A. Nakano-Doi, T. Sawano, et al., Administration of human-derived mesenchymal stem cells activates locally stimulated endogenous neural progenitors and reduces neurological dysfunction in mice after ischemic stroke, *Cells* 13 (11) (2024).
- [59] F. Guo, Y. Maeda, J. Ma, et al., Pyramidal neurons are generated from oligodendroglial progenitor cells in adult piriform cortex, *J. Neurosci.* 30 (36) (2010) 12036–12049.
- [60] M. Karow, R. Sánchez, C. Schichor, et al., Reprogramming of pericyte-derived cells of the adult human brain into induced neuronal cells, *Cell Stem Cell* 11 (4) (2012) 471–476.
- [61] H. Nishie, A. Nakano-Doi, T. Sawano, et al., Establishment of a reproducible ischemic stroke model in nestin-GFP mice with high survival rates, *Int. J. Mol. Sci.* 22 (23) (2021).
- [62] R. Nishiyama, T. Nakagomi, A. Nakano-Doi, et al., Neonatal brains exhibit higher neural reparative activities than adult brains in a mouse model of ischemic stroke, *Cells* 13 (6) (2024).
- [63] J.P. Magnusson, C. Göritz, J. Tatarishvili, et al., A latent neurogenic program in astrocytes regulated by Notch signaling in the mouse, *Science* 346 (6206) (2014) 237–241.
- [64] J.P. Magnusson, M. Zamboni, G. Santopolo, et al., Activation of a neural stem cell transcriptional program in parenchymal astrocytes, *Elife* 9 (2020).
- [65] I.S. Shimada, M.D. Lecomte, J.C. Granger, et al., Self-renewal and differentiation of reactive astrocyte-derived neural stem/progenitor cells isolated from the cortical peri-infarct area after stroke, *J. Neurosci.* 32 (23) (2012) 7926–7940.
- [66] G.H. Mochida, C.A. Walsh, Genetic basis of developmental malformations of the cerebral cortex, *Arch. Neurol.* 61 (5) (2004) 637–640.
- [67] T. Saito, S. Hanai, S. Takashima, et al., Neocortical layer formation of human developing brains and lissencephalies: consideration of layer-specific marker expression, *Cerebr. Cortex* 21 (3) (2011) 588–596.
- [68] K.I. Van Aerde, D. Feldmeyer, Morphological and physiological characterization of pyramidal neuron subtypes in rat medial prefrontal cortex, *Cerebr. Cortex* 25 (3) (2015) 788–805.
- [69] Z.M. Yao, X.R. Sun, J. Huang, et al., Astrocyte-neuronal communication and its role in stroke, *Neurochem. Res.* 48 (10) (2023) 2996–3006.
- [70] X. Wang, W. Xuan, Z.Y. Zhu, et al., The evolving role of neuro-immune interaction in brain repair after cerebral ischemic stroke, *CNS Neurosci. Ther.* 24 (12) (2018) 1100–1114.
- [71] M.R. Williamson, S.P. Le, R.L. Franzen, et al., Subventricular zone cytogenesis provides trophic support for neural repair in a mouse model of stroke, *Nat. Commun.* 14 (1) (2023) 6341.
- [72] C. Sun, H. Sun, S. Wu, et al., Conditional ablation of neuroprogenitor cells in adult mice impedes recovery of poststroke cognitive function and reduces synaptic connectivity in the perforant pathway, *J. Neurosci.* 33 (44) (2013) 17314–17325.
- [73] J. Giovanniello, K. Yu, A. Furlan, et al., A central amygdala-globus pallidus circuit conveys unconditioned stimulus-related information and controls fear learning, *J. Neurosci.* 40 (47) (2020) 9043–9054.
- [74] M.U. Woloszynowska-Fraser, P. Wulff, G. Riedel, Parvalbumin-containing GABA cells and schizophrenia: experimental model based on targeted gene delivery through adeno-associated viruses, *Behav. Pharmacol.* 28 (8) (2017) 630–641.
- [75] A. Otxoa-De-Amezaga, F. Miró-Mur, J. Pedragosa, et al., Microglial cell loss after ischemic stroke favors brain neutrophil accumulation, *Acta Neuropathol.* 137 (2) (2019) 321–341.
- [76] E.F. Willis, K.P.A. Macdonald, Q.H. Nguyen, et al., Repopulating microglia promote brain repair in an IL-6-dependent manner, *Cell* 180 (5) (2020) 833–846.e816.
- [77] R.J. Henry, R.M. Ritzel, J.P. Barrett, et al., Microglial depletion with CSF1R inhibitor during chronic phase of experimental traumatic brain injury reduces neurodegeneration and neurological deficits, *J. Neurosci.* 40 (14) (2020) 2960–2974.
- [78] B.D. Hoehn, T.D. Palmer, G.K. Steinberg, Neurogenesis in rats after focal cerebral ischemia is enhanced by indomethacin, *Stroke* 36 (12) (2005) 2718–2724.
- [79] X.S. Liu, Z.G. Zhang, R.L. Zhang, et al., Stroke induces gene profile changes associated with neurogenesis and angiogenesis in adult subventricular zone progenitor cells, *J. Cerebr. Blood Flow Metabol.* 27 (3) (2007) 564–574.
- [80] M.S. Kim, M.J. Sung, S.B. Seo, et al., Water-soluble chitosan inhibits the production of pro-inflammatory cytokine in human astrocytoma cells activated by amyloid beta peptide and interleukin-1beta, *Neurosci. Lett.* 321 (1–2) (2002) 105–109.
- [81] I.M. Fang, C.M. Yang, C.H. Yang, Chitosan oligosaccharides prevented retinal ischemia and reperfusion injury via reduced oxidative stress and inflammation in rats, *Exp. Eye Res.* 130 (2015) 38–50.
- [82] F. Bolan, I. Louca, C. Heal, et al., The potential of biomaterial-based approaches as therapies for ischemic stroke: a systematic review and meta-analysis of pre-clinical studies, *Front. Neurol.* 10 (2019) 924.
- [83] H. Huang, K. Qian, X. Han, et al., Intraparenchymal neural stem/progenitor cell transplantation for ischemic stroke animals: a meta-analysis and systematic review, *Stem Cell. Int.* 2018 (2018) 4826407.

- [84] L. Chen, H. Xi, H. Huang, et al., Multiple cell transplantation based on an intraparenchymal approach for patients with chronic phase stroke, *Cell Transplant.* 22 (Suppl 1) (2013) S83–S91.
- [85] D.J. Cook, C. Nguyen, H.N. Chun, et al., Hydrogel-delivered brain-derived neurotrophic factor promotes tissue repair and recovery after stroke, *J. Cerebr. Blood Flow Metabol.* 37 (3) (2017) 1030–1045.
- [86] D. Kalladka, J. Sinden, K. Pollock, et al., Human neural stem cells in patients with chronic ischaemic stroke (PISCES): a phase 1, first-in-man study, *Lancet* 388 (10046) (2016) 787–796.